TREC and KREC RT-qPCR screening method for primary immunodeficiencies and lymphocyte subpopulations in DiGeorge syndrome

Anna Margrét Kristinsdóttir

Thesis for the degree of Master of Science
University of Iceland
Faculty of Medicine
Department of Biomedical science
School of health Sciences

HÁSKÓLI ÍSLANDS

TREC og KREC RT-qPCR aðferð til skimunar gegn meðfæddum ónæmisgöllum og undirtýpur eitilfrumna í einstaklingum með DiGeorge heilkenni

Anna Margrét Kristinsdóttir

Ritgerð til meistaragráðu í Lífeindafræði

Umsjónarkennari: Björn Rúnar Lúðvíksson

Meistaranámsnefnd: Una Bjarnadóttir og Ásgeir Haraldsson

Læknadeild

Námsbraut í Lífeindafræði

Heilbrigðisvísindasvið Háskóla Íslands

Júní 2014

TREC and KREC RT-qPCR screening method for primary immunodeficiencies and lymphocyte subpopulations in DiGeorge syndrome

Anna Margrét Kristinsdóttir

Thesis for the degree of Master of Science

Supervisor: Björn Rúnar Lúðvíksson

Masters committee: Una Bjarnadóttir and Ásgeir Haraldsson

Faculty of Medicine

Department of Biomedical Science

School of Health Sciences

June 2014

Prentun: Samskipti ehf.

Reykjavík, Ísland 2014

Ágrip

T og B frumur sérhæfða ónæmiskerfisins gegna mikilvægu hlutverki í frumubundnu og vessabundnu ónæmi. T frumur þroskast í týmus og B frumur í beinmerg. Í þroskaferli þeirra mynda þær vakasértæka T frumu viðtaka (TCR) og B frumu viðtaka (BCR) sem eru myndaðir með genaendurröðun í þroskaferli þeirra.

Í genaendurröðun er DNA strengurinn klipptur í sundur og splæst saman aftur þannig að valin gen splæsast saman. Það sem er á milli þessara gena er klippt út úr strengnum og myndar hringlaga DNA afurð sem kallast T cell receptor excision circle (TREC) í T frumum og kappa-deleting recombination excision circles (KREC) í B frumum. TREC og KREC myndast aðeins í nýmynduðum T og B frumum og er ekki eftirmyndað þegar frumurnar skipta sér. Þar af leiðandi hefur TREC og KREC reynst góð mælieining til að greina fjölda nýmyndaðra T og B frumna í blóði.

Meðfæddir ónæmisgallar (MÓG) eru misalvarlegir arfgengir genagallar sem valda ýmist göllum í sérhæfða eða ósérhæfða ónæmiskerfinu. Í dag eru þekktir yfir 200 meðfæddir ónæmisgallar. Nýburar með MÓG líta eðlilega út við fæðingu og því eru MÓG oftast ekki greindir fyrr en einstaklingur verður fyrir alvarlegum og endurteknum sýkingum og afleiðingum þeirra, sem leiðir til dauða ef um alvarlegan MÓG er að ræða.

DiGeorge heilkenni (DGS) orsakast af 1,5-3 Mb úrfellingu á svæði 22q11.2 á litningi 22. Úrfellingin veldur afbrigðilegri myndun þriðju og fjórðu branchial pouch í fósturþroska sem getur leitt til vansköpunar á ýmsum líffærum, t.d. týmus. Afbrigðileg þroskun týmus getur svo leitt til þess að T frumu þroskun raskast sem getur valdið T frumufæð og ónæmisbresti í einstaklingum með DGS.

Rauntíma magnbundin kjarnsýrumögnun (RT-qPCR) er notuð til að mæla TREC og KREC og hefur verið innleidd í nokkrum löndum sem nýburaskimunaraðferð gegn MÓG. Þetta verkefni snérist um að setja upp þessa aðferð ásamt því að skoða undirtýpur eitilfrumna í einstaklingum með DGS. Uppsetning RT-qPCR aðferðarinnar tókst vel og niðurstöður þessarar rannsóknar sýna að einstaklingar með DGS hafa færri óreyndar T frumur borið saman við heilbrigða einstaklinga.

Abstract

T and B lymphocytes are the most critical effector cells in the adaptive immune system. T cells are developed in thymus and B cells in bone marrow. Both T and B cells express antigen specific receptors, the T cell receptor (TCR) and the B cell receptor (BCR), which are made in their developmental stages.

Diversity in the TCR and BCR repertoire is crucial for antigen recognition due to the broad antigen presentation in one's lifetime. After V(D)J recombination, a circular extra-chromosomal DNA product called T cell receptor excision circles (TREC) in T cells and kappa-deleting recombination excision circles (KREC) in B cells are formed. The TREC and KREC have shown to be a good marker for newly synthesised T and B cells since the TREC and KREC are only formed in newly synthesised T and B cells and are not replicated when T and B cells divide.

A multiplex real-time quantitative PCR (RT-qPCR) can be used to quantify TRECs and KRECs. TREC and KREC RT-qPCR has been installed in several countries as a neonatal screening programme for PIDs, as the method detects most T and B cell disorders.

Primary immunodeficiencies (PIDs) are a group of heterogeneous defects in the immune system. Over 200 PIDs disorders have been described. Most PIDs are hereditary genetic defects in the development and/or function of either the innate or adaptive immune system. Early diagnosis and treatment is crucial to prevent severe infections leading to disease-associated morbidity and mortality.

DiGeorge syndrome (DGS) is a complex syndrome caused by a 1,5-3 Mb deletion in the locus 22q11.2. The prevalence of the deletion is thought to be 1:4000. This deletion disrupts the expression of the *UFD1L* gene which causes abnormal development in third and fourth branchial pouches in embryo development, which can lead to malformations of various organs, e.g. the thymus. The disruption of the formation of the thymus leads to failure in T cell development, thus individuals with DGS are T cell lymphopenic.

TREC and KREC RT-qPCR method was setup in this study and lymphocyte subpopulations in individuals with DGS examined. The TREC and KREC RT-qPCR setup was successful and could be considered for installation as a neonatal screening programme here in Iceland. Our results demonstrate mainly reduction in naive T cell phenotypes in individuals with DGS compared to healthy controls.

Acknowledgements

.

I want to thank my supervisors, Björn Rúnar and Una, for their guidance, encouragement and for believing in me, and Ásgeir for his contribution for this study. I am very thankful for the opportunity to work at the Department of Immunology which is one of the most dynamic departments in the field of research.

So many people helped me in one way or another, and I will ever be so thankful for all the guidance and help I received in this educational journey.

I want to thank the Department of rheumatology for allowing me to use their lab and equipment, and the Department of cell biology, in particular Guðrún, for allowing me to use their equipment, even after working hours. Ásgeir at deCODE genetics inc. has my deepest gratitude for all the guidance and patient during the PCR analysis and deCODE genetics inc. for allowing me to use the ABI prism PCR machine. The Icelandic Blood bank, Jórunn and Þorbjörn, have my appreciation for their help regarding sample collection.

I will ever be so thankful for the help and patient from Inga, which helped me with the flow cytometry analysis and answered my million questions. I am also very thankful for all the help from Helga Kristín regarding both flow cytometry and statistical analysis. I want to thank Málfríður, Anna Guðrún, Helga Bjarna, Gummi and others at the Department of Immunology for their help and their kind answers to my many questions. Everybody at the department of immunology were kind and welcoming and willing to help. It was a great pleasure being a part of this great, kind and dynamic team.

My friends and family stood by me, believed in me and encouraged me. That I will ever appreciate.

And thank you fellow students at the Department of immunology for a great time.

Table of contents

Figure legends

Table legends

Abbreviations

22q11DS	22q11 deletion syndrome
Ab	antibody
ACTB	beta-actin
APC	antigen presenting cell
AT	Ataxia telangiectasia
BCD	B cell depleted
BCR	B cell receptor
BM	memory B cell
bp	basepair
BTK	burton tyrosine kinase
C	constant
cDGS	complete DiGeorge syndrome
CID	combined immunodeficiency
cj	coding joint
CVID	common variable immunodeficiency
D	diversity
DBS	dried blood spot
DGS	DiGeorge syndrome
DNA-PKcs	DNA-dependent protein kinase catalyc subunit
EDTA	ethylenediaminetetraacetic acid
FCS	forward scatter
H	heavy chain
HC	healthy control
HMG1/2	high mobility group proteins 1/2
Ig	immunoglobulin
IgAD	immunoglobulin A deficiency
IVIG	intravenous immunoglobulin
J	joining
KREC	kappa-deleting recombination excision circle
L	light chain
Lig4	ligase IV
mAb	monoclonal antibody
Mb	megabase
MHC	major histocompatability class
NHEJ	non-homologous end joining
NPV	negative predictive value
NSM	non-switched memory
PBMC	peripheral blood mononuclear cells
PBS	phosphate buffer saline
pDGS	partial DiGeorge syndrome
PID	Primary immunodeficiencies
PKU	Phenylketoneuria
PPV	positive predictive value
RSS	recombination signal sequence

RTE	recent thymic emigrants
RT-qPCR	real time quantitative PCR
SCID	severe combined immunodeficiency
scIg	subcutaneous immunoglobulin
sj	signal joint
SM	switched memory
SSC	side scatter
TBCD	T and B cell depleted
TCD	T cell depleted
TCM	central memory T cell
TCR	T cell receptor
TEM	effector memory T cell
TH	T helper cell
TREC	T cell receptor excision circle
Tregs	regulatory T cell
V	variable
VCFC	velocardiofacial syndrome
WAS	Wiscott-Aldrich syndrome
XLA	X-linked agammaglobulinemia

1 Introduction

1.1 The immune system

The immune system is a complex system where various types of molecules, cells and organs co-operate to protect the body. Under normal circumstances the immune system recognises and systematically eliminates pathogens to prevent infections. The immune system is also responsible for restoration of damaged tissue, e.g. recognition and elimination of cancer cells.

The immune system is divided into the innate and the adaptive immune system. The innate immune system is the host's first defence. The adaptive immune system is activated if the innate immune system is not able to eliminate pathogens that have entered the host´s body. The adaptive immune system is a complex system which administers antibody production and immunological memory to prevent recurrent infections and is constantly developing throughout one's lifetime. Lymphocytes are the main cellular component of the adaptive immune system. They arise from lymphoid progenitor cells in the bone marrow and are mainly divided into T cells and B cells.

1.2 T cells

T cell development takes place in the thymus. Fully developed T cells express T cell receptor (TCR) and other co-receptors, such as CD3, CD4 and CD8. T cells are double negative ($CD4^-CD8^-$) in the beginning of T cell development and have not formed their TCR. T cells migrate to the cortical region of the thymus where they receive developmental signals, which initiate gene rearrangement for TCR synthesis. The co-receptors CD4 and CD8 are then formed and T cells become double positive ($CD4^+CD8^+$, Figure 1).

T cells undergo positive and negative selection, mechanisms to ensure the release of normal and functional T cells. In positive selection the double positive T cells bind to epithelial cells in the thymus cortical region and receive signals to live and develop into single positive T cells ($CD4^-CD8^+$ or $CD4^-CD8^+$). T cells that bind to a major histocompatibility complex (MHC) class II on endothelial cells are destined to become $CD4^+$ and T cells that bind to MHC class I are destined to become $CD8^+$ T cells. T cell that are unable to bind to endothelial cells and therefore do not receive any developmental signals are eliminated via apoptosis. Positively selected T cells migrate into the medullar part of the thymus where they undergo a negative selection. Single positive T cells that bind to self-antigen presenting epithelial cells are eliminated via apoptosis. These mechanisms should prevent release of T cells programmed against self-antigens. Only 3-5% of all T cells pass through the positive and negative selection in the thymus (Starr et al., 2003). T cells leave the thymus as naive $CD4^+$ or $CD8^+$ T cells, which are T cells that have not encountered their specific antigen and have therefore not been activated (Kroger et al., 2010).

T cells need three signals for activation. The first signal is binding to an antigen presented on an antigen presenting cell (APC). The second signal is binding to a co-receptor expressed on the APC. The third signal is cytokine stimulation. T cell proliferates rapidly after activation so the amount of this specific T cell multiplies and these T cells become T effector cells.

1.2.1 T cell phenotypes

T cells can be divided into subpopulations based on their phenotype, which co-receptor they express, which cytokine they secrete and which cytokine receptors they express (Appay et al., 2008).

All T cells express CD3. T cells that also express CD4 are defined as helper T cells (T_H). The main role of T_H cells is co-stimulatory effects for various types of cells and they are very important for the humoral immunity.

T cells expressing CD3 and CD8 are defined as cytotoxic T cells (T_C). T_C cells are very important for cellular immune response as their main role is to kill virus infected cells.

Naive T cells are mature T cells that have not encountered their specific antigen and are therefore inactivated. Naive T cells express CD45RA, CCR7, CD27 and CD28, regardless of their CD4 or CD8 expression (Bateman et al., 2012). T cells start expressing CD45RO and down regulate CD45RA upon activation (McElhaney et al., 1995; Torimoto et al., 1992). Some of the naive T cell populations can be identified as recent thymic emigrants (RTEs) when expressing the RTE marker CD31 amongst CD45RA (Kimmig et al., 2002).

There are two types of memory T cells; effector memory T cells (T_{EM}) and central memory T cells (T_{CM}). T_{EM} provide protective memory as they migrate to inflamed peripheral tissues and have immediate effector function. T_{CM} are found in T cell areas in secondary lymphoid tissues and have little or no effector function but readily proliferate and differentiate to effector cells in response to antigenic stimulation (Figure 2) (Sallusto et al., 2004).

1.2.2 T cell receptor and TREC synthesis

Lymphocyte progenitors travel from the bone marrow to the thymus where they become naive T cell and their TCR is made with gene rearrangement (Ratts & Weng, 2012). During gene rearrangement the cell's DNA double strands are separated and re-joined in a systematic manner. Therefore, arranging genes in different ways contributes to the high diversity of TCR in T cells (Steffens et al., 2000).

TCR is made of two glycoprotein, alpha and beta (α and β) or gamma and delta (γ and δ). T cells can only express either doublet, α and β or γ and δ. The δ TCR gene region is located within the TCR-α gene region and therefore the expression of both glycoprotein chains is impossible (Puck, 2011; Verschuren et al., 1997). Both chains have variable part, which forms the antigen binding site and a constant part, which determines the biological activity when antigen binds to the cell´s receptor.

The TCR gene loci consists of smaller gene locus, which expresses the TCR variable part (variable, V; diversity, D; joining, J), and the TCR constant part (C). When the TCR genes are spliced together, the genes in between the splices are cut out from the DNA strand and form a circular extra-chromosomal DNA product, called T cell receptor excision circles (TREC) (Bains et al., 2009; Puck, 2011, 2012). The circular structure of the extra-chromosomal DNA product makes it stable and protected against DNA degradation enzymes.

The first rearrangement of the αTCR occurs between δRec-ψJα, forming a signal joint (sj) TREC. The second rearrangement occurs between Vα and Jα and forms coding joint (cj) TREC (Figure 1).

About 70% of all T cells produce this δRec-ψJα sjTRECs (Serana et al., 2013). Therefore, the δRec-ψJα sjTRECs is the most widely used biomarker for measuring TRECs levels and RTEs (Douek et al., 1998; Routes et al., 2009; Steffens et al., 2000). TRECs are only formed when the TCR is formed and are not replicated within cell division. Therefore are TRECs thought to be a good marker to quantify RTEs (Puck, 2011, 2012).

Thymus tissue and function decreases with age. Consequently, the number of RTEs and the amount of TRECs decreases and the ratio of TRECs to total T cells decreases (Bains et al., 2009; Borte et al., 2011). Neonates have very high proportion of RTEs and hence a high ratio of TRECs per total T cells. Neonates receive maternal T cells in gestation, which would give false high total T cell count in blood samples. Maternal T cells do not produce TRECs and therefore TRECs measurements do not give false high total T cell count in neonates. Neonates born before 40 weeks of gestation have fewer T cells than those born after full gestation because their immune system is not fully mature (Nakagawa et al., 2011; Puck, 2011).

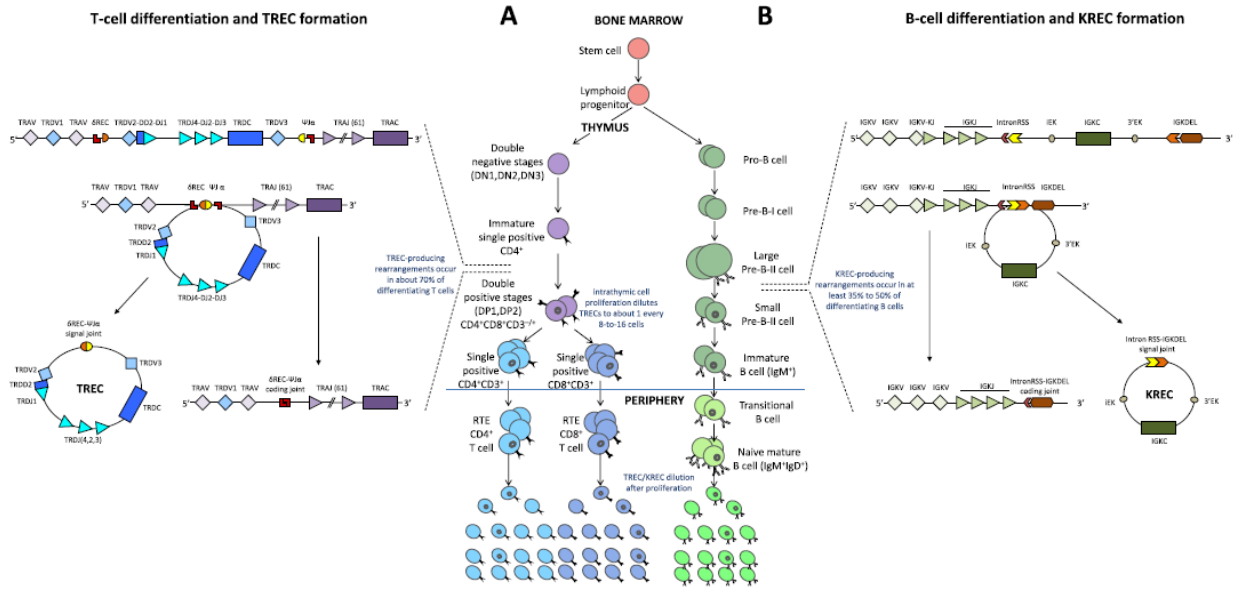

Figure 1. T and B cells differentiation and TREC and KREC synthesis (Serana et al., 2013).

1.3 B cells

B cells arise from lymphoid progenitor cells in the bone marrow. Their development takes place in the bone marrow where their B cell receptor (BCR) is made with gene rearrangement.

The lymphoid progenitor cell differentiates into pro-B cell and rearranges the immunoglobulin (Ig) heavy chain locus. If the rearrangement is successful, the pro-B cell maturates into a pre-B cell. In the pre-B cell stage, the light chain is rearranged. The light chain can be rearranged several times until a functional one gives rise to immature B cells expressing IgM BCR. B cells leave the bone marrow as transitional B cells (immature B cells) and travel throughout the body with blood and fluids to secondary lymphoid organs (Marie-Cardine et al., 2008). Transitional B cells that bind to a self-antigen

will undergo apoptosis. B cells that do not bind to self-antigens differentiate into mature naive B cells and activates upon binding to a cognate antigen. Activated naive B cells proliferate, internalize the antigen via the BCR and both process and present antigen derived peptides on MHC class II. Through the course of the germinal centre reaction, the B cells proliferate and daughter cells rearrange the BCR locus, resulting in class-switching (from IgM and IgD to either IgG, IgA or IgE) and introduction of non-germline encoded nucleotides that result in unique BCR specificities. Each new daughter cell tests its BCR for affinity on follicular dendritic cells (DCs), and those with higher affinity survive. This process is referred to as somatic hyper mutation and affinity maturation. A subset of the activated B cells further differentiates into memory B cells (B_M) or plasma cells. Memory cells can respond faster and with greater magnitude than their naive counterparts as they have higher affinity BCR. Plasma cells are the final stage of B lineage development and travel to the bone marrow (or, in some cases, stay in the secondary lymphoid organs) where they can produce antibodies for many years. If an optimal survival niche is not found the plasma cells will be short lived. The plasma cell is optimally designed to produce large amounts of antibody molecules. It should be noted that, in some cases where multivalent antigens can cross-link the BCR efficiently, T cell help is not required for antibody production, although germinal centres are not typically formed. B cells that are auto-reactive are deleted with apoptosis or their BRC is edited, or the B cells become anergic.

Activated B cells can sense innate stimuli, process and present antigens to T cells and produce pro- and anti-inflammatory cytokines. Activated B cells can also become plasma cells, which produce and secrete high affinity antibodies. The antibody produced by plasma cells has exactly the same structure and specificity as the immunoglobulin receptor it expresses (Pieper et al., 2013).

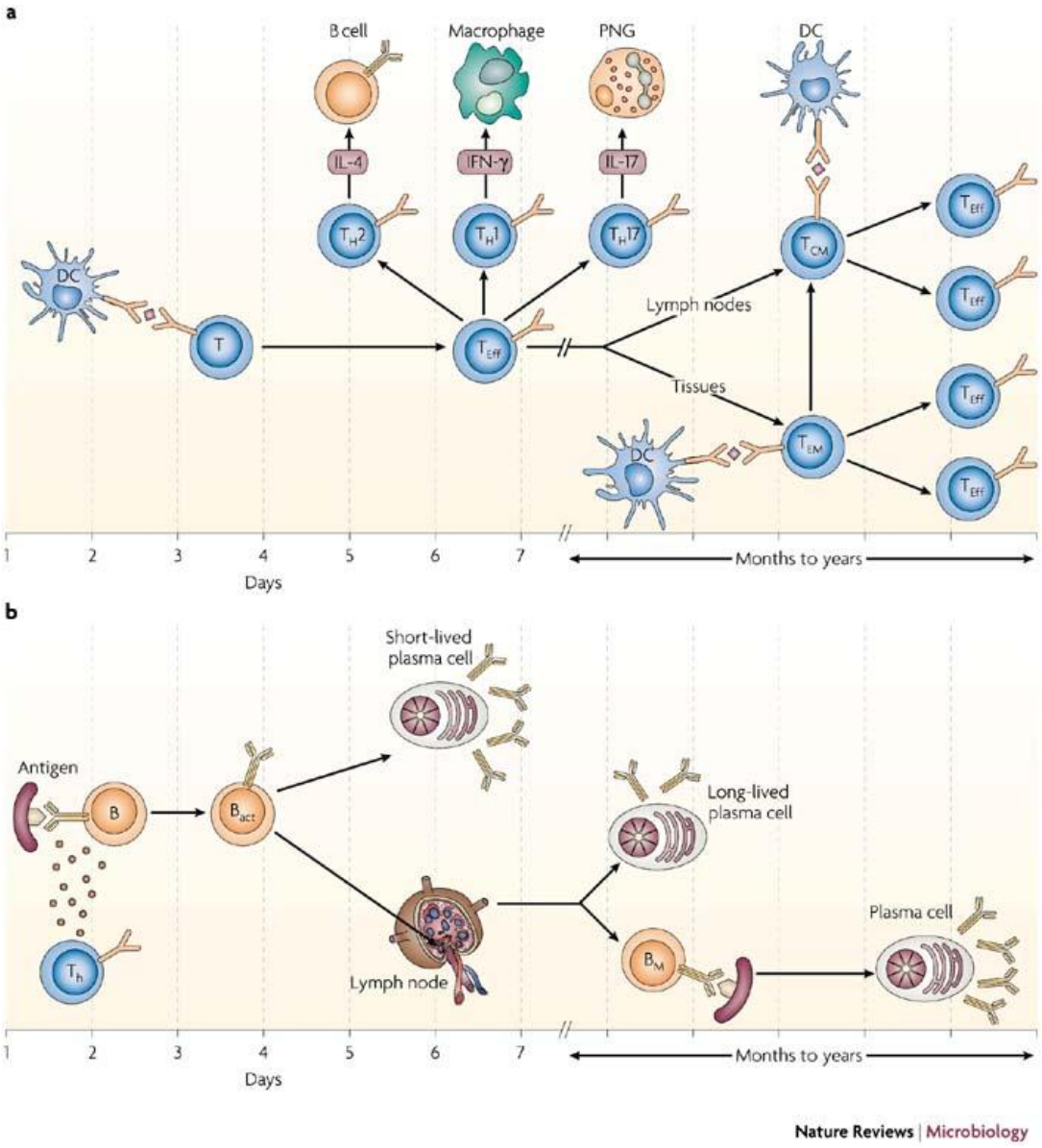

Figure 2. a) The T cell and b) the B cell differentiation (Kaufmann, 2007).

1.3.1 B cell receptor and KREC synthesis

BCR is a membrane bound immunoglobulin (Ig) made from two identical heavy (H) polypeptide chains, two identical light (L) polypeptide chains and has both a variable part (V) and a constant part (C). The antigen binding site is located at the variable part. BCR constant part determines the cell bioactivity and function. BCR is highly variable between cells so each person develops a wide range of BCR repertoire and is therefore capable of recognizing almost any antigen (Pieper et al., 2013).

There are five types of H polypeptide chains (α, δ, ε, γ and μ) and Ig are divided into five categories according to the H chains; IgA, IgD, IgE, IgG and IgM. There are two types of Ig L chains, lambda (λ) and kappa (κ). Ig is made of only one type of L chain and one type of H chain. 60% of B cells in human express κ and 40% express λ (Brauninger et al., 2001).

BCR gene region is divided into V, D and J for the heavy chain and V and J for the light chain. First the D_H and J_H are spliced together and the cell becomes early pre-B cell. V_H is then spliced with the D_HJ_H part and the cell becomes late pro-B cell generating μ H chains (Pieper et al., 2013). The μ chain binds to a surrogate L chain to form a pre-BCR, which is transported onto the cell membrane in order for the cell to check whether the newly formed H chain is functional. Furthermore, the binding prevents further rearrangement on the second IgH allele, a mechanism called allelic exclusion. The B cell has become a large pre-B cell and B cells with functional BCR enlarges and proliferates (Almqvist & Martensson, 2012; Pieper et al., 2013). After the cell division, the B cell becomes small pre-B cell and begins to rearrange the L chain gene locus. The L chain binds to the H chain and forms the BCR, which is transmitted onto the cell´s membrane and the cell becomes immature B cell. Immature B cell´s BCR is either IgD or IgM (Treanor, 2012).

κ-deleting recombination excision circles (KRECs) is synthesised when the BCR is formed and is similar to the formation of TRECs. Coding joint KRECs (cjKRECs) are formed when VDJ gene rearrangement occurs and are not exported out of the DNA strand. Signal joint KRECs (sjKREC) are formed in a latter rearrangement and are exported out of the DNA strand. The cjKRECs are replicated during cell division whereas sjKRECs are not exported out of the DNA strand. Therefore, sjKRECs is degraded in each cell division and has been proven to be a good marker for newly synthesised B cells (Kroger et al., 2010; van Zelm et al., 2007).

1.4 V(D)J recombination in T and B cells

Diversity in T and B lymphocyte receptor repertoire is crucial for antigen recognition due to the broad antigen presentation in one's lifetime. The repertoire diversity is due to somatic gene rearrangement commonly known as V(D)J recombination, a precise mechanism controlled and maintained by various DNA enzymes and proteins. V(D)J recombination in the H and L chain of the Ig BCR versus the recombination in αβ or γδ TCR is very similar.

V(D)J recombination occurs in two phases, a cleavage phase and a joining phase. The cleavage phase involves the breakdown of the DNA double strand, which is controlled by the lymphoid specific recombinases; RAG-1 and RAG-2 and recombination signal sequences (RSSs). RSSs are conserved non-coding DNA sequences flanked to the antigen receptor gene coding elements. The RSS consists of a heptamer, a spacer and a nonamer. The heptamer is a conserved seven nucleotide sequence always contiguous with the 3´ end of a coding sequence, the nonamer is a conserved nine nucleotide segment adjacent to the 5´ end of the coding segment and the spacer is either a 12±1 or 23±1 base pair (bp) long, non-conserved, segment in between the nonamer and heptamer (Brandt & Roth, 2004; Lee et al., 2003; Schatz & Swanson, 2011). Gene coding segment flanked to a 12RSS (RSS with 12 bp spacer) can be joined only to one flanked by a 23RSS (RSS with 23 bp spacer), requirement known as the 12/23 rule, although there are exceptions to this rule (Jung & Alt, 2004; Lee et al., 2003).

The cleavage phase begins with the binding of RAG-1/RAG-2 and high mobility group proteins 1/2 (HMG1/2) to an RSS flanking a coding sequence, where RAG-1 binds to the nonamer and the heptamer is the site of the DNA cleavage. A single RAG:RSS complex is thought to bring another RAG:RSS complex into close proximity, embracing the 12/23 rule (Lee et al., 2003). RAG-1 and RAG-

2 have an endonuclease activity, cutting the phosphodiester bond of the DNA backbone precisely between its coding segments and flanking RSS and thus creating a 3´-hydroxyl (OH) end on the coding segment. The 3´-OH end reacts with the phosphodiester bond on the opposite DNA strand with transesterification reaction, thus creating a double strand break with a pair of DNA hairpin loops at the coding end, and a signal end with a pair of blunt 5´-phosphorilated DNA end at the heptamer of the RSS (Brandt & Roth, 2004; Lu et al., 2008; Murphy et al., 2008; Schatz & Swanson, 2011).

In the joining phase, DNA ends are re-joined when DNA is modified by adding or subtracting nucleotides (Agard & Lewis, 2000). After cleavage the coding and signal ends are bound to the RAG complex. The coding end dissociates while the signal end remains tightly bound to the RAG complex (Brandt & Roth, 2004; Schatz & Swanson, 2011). The binding of the signal end to the RAG complex stimulates non-homologous end joining (NHEJ) repair mechanism (Lee et al., 2004). The NHEJ repair mechanisms consist of various proteins; Ku70, Ku80, XRCC4, DNA ligase IV (Lig4), DNA-dependent protein kinase catalyc subunit (DNA-PKcs) and Artemis. Ku70 and Ku80 form an end binding heterodimer, which recognizes broken ends and is thought to recruit other NHEJ proteins such as XRCC4 and Lig4. XRCC4 and Lig4 form an end-ligation complex which catalyses the ligation step. Artemis are only required for coding ends where DNA-PKcs activate an endonuclease activity in Artemis, which cleaves coding end hairpins and is also thought to contribute to junctional deletion of nucleotides (Figure 3)(Jung & Alt, 2004).

The two signal ends are joined perfectly, without loss of nucleotides and form a circular DNA product. The signal joint forming is beneficial as the reactive 3´-OH ends is neutralized to prevent further joining events (Brandt & Roth, 2004). Although signal joints are generally lost during cell division, they do have RSSs within and the RAG proteins attached so they can undergo further recombination which can cause genomic instability in thymocytes (Neiditch et al., 2002). Signal joints are retained in the chromosome in some cases to preserve chromosomal integrity. The recombination is inversional and signal ends are joined to one another rather than to target DNA so the result is the same, weather signal joint is excised or retained on the chromosome (Brandt & Roth, 2004).

Although V(D)J recombination generates mainly coding and signal joints, there are two other types of products which can be formed with nonstandard V(D)J recombination in the absence of NHEJ proteins. The former ones are hybrid joints, which forms when a RSS is joined to the coding segment of its partner RSS. The latter ones are open-and-shut joints, which form when the same pair of coding and signal ends is cleaved and re-joined (Bassing et al., 2002; Brandt & Roth, 2004).

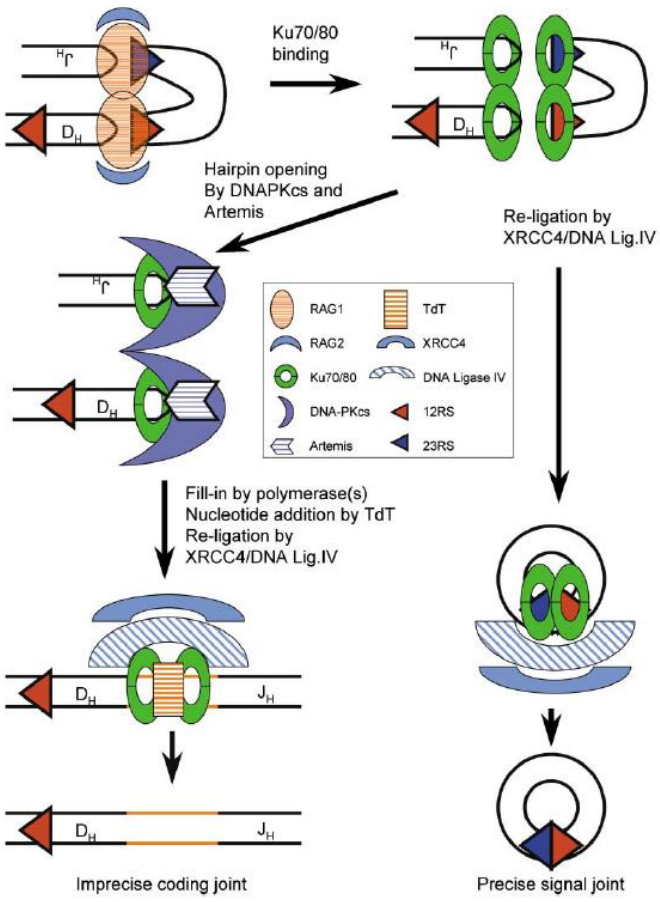

Figure 3. The cleavage and joining phase in DNA double strand brake repair mechanism (Jung & Alt, 2004).

1.5 Primary immunodeficiencies

Primary immunodeficiencies (PIDs) are a group of heterogeneous defects in the immune system. Most PIDs are hereditary genetic defects in either the innate or adaptive immune system development and/or function (McCusker & Warrington, 2011). Over 200 primary immunodeficiency disorders have been described (Borte et al., 2011). The prevalence for all PID´s is approximately 1 in 1200 live births in the USA and the most common PID is IgA deficiency with the prevalence of 1 in 300 to 500 live births. The most common clinical presentation amongst all PIDs is increased susceptibility to infections. The clinical presentation, severity of infections, diagnosis, treatment and prognosis for PIDs is highly variable between each defect. Early diagnosis and treatment is crucial for the more severe types of PIDs to prevent severe infections leading to disease-associated morbidity and mortality. Individuals with PID need sometimes both supportive and definitive treatments, like intravenous (IGIV) or subcutaneous (scIg) Ig replacement therapy, antibiotic and antifungal prophylaxis, bone marrow transplantation and hematopoietic stem cell transplantation (McCusker & Warrington, 2011). PID classification is listed in Figure 4.

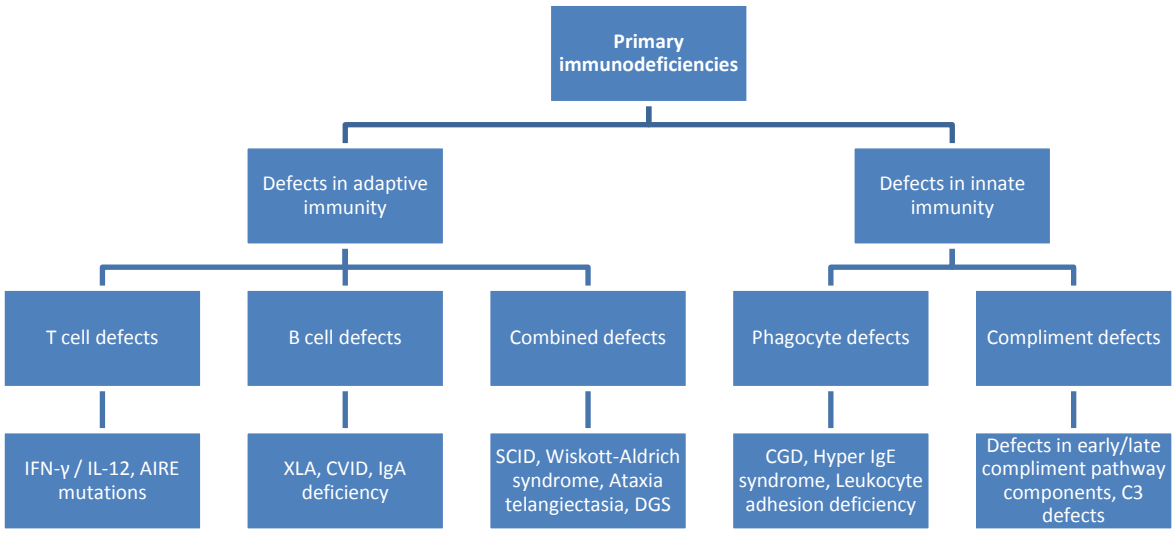

Figure 4. Classification of primary immunodeficiency.

1.5.1 Disorders of adaptive immunity

Defects in T cells development, differentiation and maturation leads to cellular immunity disorders. Individuals with T cell defects are often lymphopenic (abnormally low levels of lymphocytes) and neutrophenic (abnormally low levels of neutrophils) even though normal T cell counts do not exclude the possibility of T cell defects where the T cells could be non-functional. Individuals with T cell defects are often susceptible to opportunistic pathogens, e.g. *Candida albicans* (McCusker & Warrington, 2011).

Defects in B cell development and/or maturation lead to disorders in humoral immunity where the serum Ig levels are reduced or absent or the Ig have abnormal function. More than 20 B cell defects have been defined and are the most common form of PID´s, comprising about 50% of all PID diagnoses. Individuals with B cell defects are often diagnosed after 6 months of age. Therefore, they have increased susceptibility to respiratory tract infections and tend to be more vulnerable to capsulated bacteria (McCusker & Warrington, 2011; van Zelm et al., 2011).

Combined immunodeficiency (CID) is a form of PID where both the cellular and humoral immune systems are defected. T cells are crucial cytokine source for B cell development and maturation so CID can occur from either defects in T cells or from defects in both T and B cells (McCusker & Warrington, 2011).

In the mid-1980s, IVIG (intravenous immunoglobulin) came into common use. This treatment allowed patients to achieve normal or near normal concentrations of IgG (Conley et al., 2005).

1.5.1.1 SCID

Severe combined immunodeficiency (SCID) is a severe congenital immune defect where the individual produce no or very few active or inactive lymphocytes (Puck, 2011). Neonates with SCID seem healthy at birth where they are protected by their maternal IgG from gestation. Several months after birth they need to rely on their own immune system and get severe infections caused by opportunistic

pathogens, which their impaired immune system cannot overcome. The opportunistic pathogens cause thrush, pneumonia and diarrhoea in SCID individuals if untreated (Puck, 2012). SCID condition is not viable if individuals are not treated. Therefore early diagnosis is very important, before onset of serious infections and their consequences. Preferable SCID therapy (though disease phenotype dependant) is hematopoietic stem cell transplantation from a healthy donor. Hematopoietic stem cell transplantation is considered to be most effective if it is done before three months of age (Puck, 2011; Routes et al., 2009).

Over 20 genetic defects are known causes of SCID, characterized by severe defects in both cellular and humoral immunity. In some cases, genetic SCID is observed when a child deceases because of severe infections that were not adequately diagnosed and treated early enough. In other cases, infants and even unborn children have been diagnosed with SCID where the SCID is known to run in their families, which implies early treatment and good life expectancy (Puck, 2012). Some studies show that over 80% of SCID cases are not hereditary (Chan et al., 2011). In the USA, the prevalence of SCID is estimated 1:50,000–100,000 (Puck, 2011).

SCID is generally categorized according to the lymphocyte presentation, i.e. whether there is an absence of T cells but presence of B cells (T^-B^+) or absence of both T and B cells (T^-B^-). The genetic phenotype of SCID can also be determined according to the NK cell count (McCusker & Warrington, 2011).

1.5.1.2 DiGeorge syndrome

DiGeorge syndrome (DGS) is a complex syndrome caused by deletion of chromosome 22, specifically 1,5-3 mega base (Mb) deletion of locus 22q11.2 (Lima et al., 2010; Pierdominici et al., 2003). This deletion also causes velocardiofacial syndrome (VCFC), which is named after the most common visible symptoms of the syndrome, which are defects in velopharyngeal port (cleft lip and cleft palate) and hart defects. These syndromes often interweave and are called 22q11 deletion syndrome (22q11DS) for simplicity (Cancrini et al., 2005; Oskarsdottir et al., 2005; Pierdominici et al., 2003). The 22q11DS is the most common disease caused by gene deletion and is considered to be an autosomal dominant genetic disease, although the majority of cases seem to be stochastic ("*de novo*") and not inherited (Oskarsdottir et al., 2005; Pierdominici et al., 2003). The frequency of the deletion is estimated to be 1:4000 (Jawad et al., 2011; Oskarsdottir et al., 2005; Yu et al., 2012). About 90% of individuals diagnosed with DGS have the 22q11.2 deletion and often hemizygous deletion (Hsieh et al., 2012; Markert et al., 1998; Pierdominici et al., 2003). This deletion disrupts the expression of the *UFD1L* gene which causes abnormal development in third and fourth branchial pouches in embryo development, which can lead to malformations of various organs, e.g. the thymus (Hsieh et al., 2012; Markert et al., 2004b). A range of clinical symptoms such as; thymic aplasia, hypocalcaemia, speech difficulties, velopharyngeal malformations (cleft lip and palate), developmental impairment, learning disabilities and behavioural problems can be observed with various severity (Jawad et al., 2011; Lima et al., 2010; Oskarsdottir et al., 2005). Swedish DGS study from 2004 revealed that most subjects (74%) were diagnosed after two years of age. Individuals who are diagnosed before two years of age had severe heart defects that lead to DGS diagnosis. Immunosuppression, speech problems, glitches

in the palate, developmental impairment and learning disabilities led to diagnosis in older children (Oskarsdottir et al., 2005).

Thymic aplasia or thymic hypoplasia in individuals with deletion of the 22q11.2 causes immunosuppression and abnormal or no functional T cells. Immunosuppression varies between individuals and does not necessarily correlate to the thymic phenotype (McLean-Tooke et al., 2011).

DGS is divided into complete (cDGS) and partial DGS (pDGS) based on the severity of the immune deficiency. cDGS is far less common than pDGS (Markert et al., 2004b; Markert et al., 1998). cDGS individuals have no or very few T cells in their blood (0-2%) or no T cells who response to mitogen stimulation for cell proliferation. cDGS is severe and preferable treatment is thymic or bone marrow transplantation (Cancrini et al., 2005; Markert et al., 1998; Pierdominici et al., 2003). pDGS individuals have normal or few T cells in their circulation and/or reduced T cell proliferation (Cancrini et al., 2005). Immunosuppression in pDGS individuals can improve over time, probably due to the fact that some T cells are present and can proliferate (Cancrini et al., 2005; Hsieh et al., 2012; Markert et al., 1998; McLean-Tooke et al., 2011). Atypical cDGS has also been described as condition where genetic disorder is not present. Individuals with atypical cDGS can form T cells that are different from normal T cells since they have much less diversity in TCR repertoire, do not express CD45RA and CD62L, do not form TRECs and may not response to mitogen stimulation. This condition is thought to arise from abnormal T cell positive and negative selection in thymus (Markert et al., 2003).

1.5.1.3 Wiskott-Aldrich syndrome

Wiskott-Aldrich syndrome (WAS) is a rare X-linked inherited PID caused by mutations in the WAS gene. WAS protein is expressed in hematopoietic cells and regulates the cytoskeleton (Castiello et al., 2013; Matalon et al., 2013). The mutations lead to the absence of functional WAS protein, which leads to a severe clinical phenotype, that can result in death if not diagnosed and treated early in life, preferably with hematopoietic stem cell transplantation. The disease is characterized by microthrombocytopenia, eczema, recurrent infections, and an increased prevalence of autoimmunity and malignancies (Massaad et al., 2013).

1.5.1.4 Ataxia telangiectasia

Ataxia telangiectasia (AT) is an autosomal recessive inherited disease characterized by progressive cerebellar ataxia, immune defects, oculocutaneous telangiectasia and predisposition to malignancies (Jacquemin et al., 2012). AT is caused by mutations in the *ATM* gene, a gene coding for ataxia telangiectasia mutated protein kinase. The ATM protein kinase is 370 kDa and has major functions in the cellular response to DNA damage, e.g. double strand brake repair. The phenotype and severity of AT has shown to be correlated to the genotype and size of the mutations in the *ATM* gene. Patients with biallelic truncating mutations of the ATM gene have no functional ATM protein kinases and have immunodeficiency and neurodegeneration. Patients with either leaky splice site or missense mutations express some functional ATM protein kinases resulting in milder neurological presentation and/or slower rate of neurodegeneration and often no immunodeficiency (Staples et al., 2008). Individuals with AT have low TREC and borderline KREC values (Borte et al., 2012).

1.5.1.5 X-linked agammaglobulinemia

X-linked agammaglobulinemia (XLA) is one of the most common PIDs and is, like the name specifies, an X-linked recessive disease. All males that have a mutated X chromosome will display symptoms of the disease (Conley et al., 2005). XLA is caused by mutations in the Burton´s tyrosine kinase (*BTK*) gene (Martini et al., 2011). There are over 800 mutations that have been reported to affect *BTK* and no single mutations accounts for more than 3% of patients (Conley et al., 2005). The mutations block the maturation of B cells at the pre-B cell stage which leads to impairment in the B cell development and severe reduction of mature B lymphocytes. The severe reduction of mature B lymphocytes leads to reduced serum Ig of all subclasses and no specific antibody responses (Martini et al., 2011; Mohamed et al., 2009). The few peripheral B cells that individuals with AT have exhibit an immature IgM phenotype (Conley et al., 2005; Martini et al., 2011). The main therapy for XLA patients is gammaglobulin replacement (Conley et al., 2005).

Individuals with XLA have normal TREC and low KREC values (Nakagawa et al., 2011).

1.5.1.6 Common variable immunodeficiency

Common variable immunodeficiency (CVID) is the most common symptomatic PID with estimated prevalence of 1:25.000 (Ameratunga et al., 2013). Approximately 10% of CVID cases are inherited and the genetic cause has yet not been identified (Chapel et al., 2008; Salzer et al., 2012). CVID is characterized of reduced serum levels of IgA, IgG and IgM, recurrent and/or severe infections, autoimmunity, malignancy and allergic disorders and individuals become symptomatic in their adulthood (Cunningham-Rundles, 2012). About 40-50% of CVID patients have slightly reduced peripheral B cells (Salzer et al., 2012). The treatment of choice for CVID is lifelong IVIG or scIg replacement (Ameratunga et al., 2013).

Neonates with CVID have normal TREC and KREC values (Borte et al., 2012) while adults seem to have low TREC and KREC values (Serana et al., 2013).

1.5.1.7 IgA deficiency

IgA deficiency (IgAD) is the most common type of PID with the prevalence of 1:600 in Caucasian. Familial inheritance occurs in about 20% of cases (Hammarstrom et al., 2000). The genetic basis of IgAD has not yet been clarified. Individuals with IgAD lack IgA in both serum and mucosal tissues but have normal values of other Ig isotypes (Pandolfi et al., 2010; Yel, 2010). Individuals with IgAD are often asymptomatic, but symptoms correlated to IgAD are respiratory and gastrointestinal tract infections and non-infectious symptoms, e.g. celiac disease, allergic and autoimmune diseases (Singh et al., 2014).

Individuals with IgAD have normal TREC and KREC values (Borte et al., 2012).

1.5.2 Disorders of innate immunity

The innate immune system´s defence mechanism is recognition and elimination of threatening organisms with phagocytes (neutrophils and macrophages), DCs and complement proteins. Defects in the development or function of any of these compartments may lead to failure of the innate immune system to recognize and eliminate pathogens to prevent infections, which may in return lead to PIDs.

Individuals with innate immunodeficiency disorders present symptoms, such as recurrent infections, at any age (McCusker & Warrington, 2011).

1.6 Neonatal screening programme

Neonatal screening is a screening programme which each country or state determines and maintains, to screen for certain diseases in all neonates born in their district. Neonatal screening programme makes it possible to map the diseases and calculate new estimate prevalence, leads to early treatment and thereby increasing the life quality and expectancy for the patients. Neonatal screening is important to diagnose patients with serious diseases where the patients would perhaps not be diagnosed until severe and life-threatening symptoms or consequences have occurred.

Most neonatal diagnosis nowadays use a sampling method that Robert Guthrine discovered in 1963 in order to detect phenylketonuria (PKU) in neonates. The neonate´s heel is pricked and blood drops are dripped onto filter paper, often called Guthrine card (Puck, 2011) or dried blood spot samples (DBS). The filter paper has many benefits. It is easy to handle, can be stored for many years at right conditions (-20 °C) and can easily be transported between places. An important factor in the development of a new diagnostic method for neonatal screening is to use the same sample method already used in neonatal screening to avoid other unnecessary and uncomfortable sampling methods (Puck, 2012).

1.6.1 The Icelandic neonatal screening programme

The Icelandic neonatal screening programme is similar to other Nordic countries and the USA programme, i.e. screening for serious congenital metabolic diseases. DBS samples are prepared as described previously (Franzson et al.).

1.6.2 Primary immunodeficiency neonatal screening programmes abroad

Screening programme for PIDs in neonates has been installed as a routine screening programme, for example in Sweden and in several states in the USA. In the USA various analytical methods to detect immunodeficiency were discussed for installation of the screening programme. However, too extensive blood sampling was needed for these methods compared to the DBS samples. Furthermore, the specificity nor the sensitivity were good enough and therefore they were not convenient candidates as neonatal screening methods (Puck, 2011). At first it was planned to analyse immunodeficiency in neonates by counting lymphocytes in whole blood. Lymphocytes in neonates are estimated to be 5000/µl whole blood, of which T-cells are 70% of the total count. Disadvantages in counting lymphocytes in neonatal whole blood are that the method detects all lymphocytes in the sample and would therefore give false high lymphocyte counts as neonates can have maternal lymphocytes. Furthermore, absolute cell count would not detect the ratio of T, B and NK cells. (Puck, 2012).

1.6.2.1 The neonatal screening programme in Sweden

A multiplex real-time quantitative PCR (RT-qPCR) method is used to quantify TRECs and KRECs in neonatal DBS samples in Sweden. The house-keeping gene, β-actin (ACTB) is also measured as a reference to evaluate the success of the DNA elution and the RT-qPCR procedure. The ACTB gene is

a constant gene expressed in every cell where the gene encodes the actin structural protein of the cytoskeleton and is considered a good choice as a reference gene in PCR (Wang et al., 2012).

Normal TREC, KREC and ACTB values in neonates after full gestation is ≥8 TREC copies/μL, ≥6 KREC copies/μL and ≥1000 ACTB copies/μL. Low ACTB results indicate a failure in either the DNA elution and/or the RT-qPCR procedure so the results are considered inconclusive. Abnormal results (low TREC or KREC values) require repeated testing and/or DNA elution (Borte et al., 2012).

2 Aims

The main aims of this study were to finish the installation and adjust the RT-qPCR analysis method to quantify TRECs and KRECs in neonatal DBS samples and examine the immunophenotypic profile in individuals with DiGeorge syndrome. The specific aims were:

1. Setup a DNA elution method for DBS samples.
2. Test the RT-qPCR method by analysing approximately 1200 neonatal DBS samples and compare our results with previously published results in order to compare the specificity and sensitivity.
3. Examine the lymphocyte subpopulations in individuals with DGS using flow cytometry analysis in order to see if the DGS subjects have different relative sizes of subpopulations compared to healthy controls.
4. Examine serum Ig levels in individuals with DGS and compare the results to the B cell subpopulation results from flow cytometry analysis.

3 Material and methods

3.1 Study design

DNA was eluted from DBS samples. RT-qPCR was performed on neonatal and DGS DBS in order to quantify TRECs, KRECs and ACTB using an absolute quantitative method with standard curve. Samples from individuals with DiGeorge syndrome were analysed with flow cytometry for immunophenotyping. Ig levels were also examined with quantitative nephelometry in these samples.

The RT-qPCR part of this study was in collaboration with Dr. Lennart Hammarstöm (Department of Laboratory Medicine, Karolinska Institute, Stockholm, Sweden) and Dr. Stephan Borte (Translational Centre for Regenerative Medicine, Leipzig, Germany). The collaborative parties provided fully functional protocols for DBS DNA elution and RT-qPCR. Both the DNA elution and RT-qPCR were performed strictly according to the protocols, e.g. using the recommended reagent solutions and instruments. The collaborative parties are in collaboration with many other European countries to setup the TREC and KREC neonatal screening programme identically within these countries.

The study was approved by the ethical committee of Landspítali, The National University Hospital of Iceland (Ref. nr. VSNb2012110043/03.07) and the Data Protection Authority (Ref.nr. 2012121424HGK/--).

3.2 Study subjects and sample collection

Study subjects were in three parts. The first part contained 30 healthy volunteers from the Icelandic Blood Bank. Blood bank volunteers have to be: 18-60 years of age, weight more than 50 kg and not receiving any drugs. Samples were taken after obtaining written consent. Four whole blood drops were dripped onto Whatman903^{TM} filter paper.

The second part of the study subjects contained 1200 neonatal DBS samples from heel puncture, dripped onto Whatman903^{TM} filter paper obtained from the Department of Genetics and Molecular Medicine, Landspítali, The National University Hospital of Iceland.

The third part of the study subjects contained 6 individuals previously diagnosed with DiGeorge syndrome with 22q11.2 deletion. The DiGeorge group consisted of three males and three females, from age 12 to 44. Eight mL of blood was collected in ethylenediaminetetraacetic acid (EDTA) Vacuette vacutainer for flow cytometry analysis, four mL of blood were collected in Serum Sep Clot Activator Vacuette vacutainer for nephelometry analysis and four whole blood drops were dripped onto Whatman903^{TM} filter paper for the RT-qPCR analysis.

Three of the DGS subjects are an exception from the description above. For those DGS subjects, blood was collected only in EDTA Vacuette vacutainer. Peripheral blood mononuclear cells (PBMCs) were isolated from whole blood using ficoll density separation and EDTA whole blood was used for DNA extraction and TREC and KREC RT-qPCR analysis. These DGS subjects were not included in the nephelometry analysis as no blood serum was collected.

3.3 DNA elution from dry blood spot samples

DNA was eluted from single 3,2 mm Whatman 903™ dried blood spot punch. One 3,2 mm DBS is estimated to be equal to three µL of whole blood. DNA from DBS was eluted according to the following protocol from the collaboration parties. The protocol has been optimised for use with FrameStar® 96 semi-skirted clear PCR plate (4titude Ltd., UK).

One DBS was placed in each well of a 96 well plate. The samples were purified by adding 80 µL of Generation DNA Purification Solution (Qiagen, Hilden, Germany) to each well. Plates were centrifuged until reaching 2000 rpm and incubated for 10 minutes at room temperature (RT). Plates were then centrifuged at 3500 rpm for five minutes and all liquid removed from each well afterwards. This purification routine was repeated once. All samples were washed once by adding 80 µL of milliQ water to each well and plates centrifuged until reaching 2000 rpm. 20 µL of Generation DNA Elution Solution (Qiagen), supplemented with 10 ng/mL yeast tRNA (Invitrogen™, CA, USA), was added to each well using low-retention/binding tips. Samples were sealed with Optical adhesion covers (Applied Biosystems®, Foster City, CA, USA) and heat-eluted in 2720 Thermal Cycler (Applied Biosystems®) at 99°C for 30 minutes. Plates were cooled down, rigorously vortexed and centrifuged until reaching 2000 rpm. Plates were stored at 4°C for same-day analysis or -20°C for longer period.

3.4 DNA concentration measurements

DNA concentration and purity was measured in all samples from healthy adult blood donors using NanoDrop® ND-1000 UV/Vis spectrophotometer (NanoDrop technologies, Inc., Wilmington, DE) to access the assurance of the DNA elution method. Nanodrop calculates DNA concentration according to modified Beer-Lambert equation (1). One µL of sample was measured at 260 nm and distilled water used as blank. DNA concentration was given in ng/µL.

$$C(A \times \varepsilon)/\mathrm{b}$$

Equation 1. c is the nucleic acid concentration in ng/µL, A is the absorbance in AU, ε is the wavelength-dependent extinction coefficient in ng-cm/µL and b is the path length in cm

3.5 TREC and KREC RT-qPCR

RT-qPCR was performed using ABI PRISM® 7900HT (Applied Biosystems®) owned by deCODE genetics, Reykjavik, Iceland.

The collaborative parties provided pre-prepared PCR master mix, standard samples and control samples manufactured by the Translational Centre for Regenerative Medicine, Leipzig, Germany. The PCR master mix contained specific oligonucleotides and hydrolysed probes for TREC, KREC and ACTB specific detection. TREC probes were labelled with FAM fluorochrome, KREC probes labelled with VIC fluorochrome and ACTB probes labelled with NED fluorochrome. The master mix also contained $MgCl_2$, bovine serum albumin (BSA), ROX dye, *E.coli* uracil-DNA glycosylase (UDG) and specific dUTP:dTTP nucleotide ratio.

Five standard samples were analysed in order to make a standard curve. The standard samples were in a tenfold dilution, from 100.000 to 10 copies/µL for TREC and KREC and from 1.000.000 to 100 copies/µL for ACTB. The two least concentrated standard samples were analysed in triplicates and higher standard samples in duplicates. Five control samples were analysed in each RT-qPCR run, normal control (NC), T cell depleted sample with no TREC (TCD), B cell depleted sample with no KREC (BCD), T and B cell depleted sample with neither TREC nor KREC (TBCD) and no template control sample with no DNA present (NTC-PCR).

12 µL of the PCR master mix and 8 µL of sample were added to each well of a white 384 well PCR plate (Thermo scientific, MA, USA) with low retention/binding SafeSeal Tips (Biozym scientific GmbH, Hess. Oldendorf, Germany). Plates were sealed with Optical adhesion covers (Applied Biosystems® before inserted into the ABI PRISM® 7900HT (Applied Biosystems®).

The thermal cycle program is shown in Table 1. The first step was UDG activation at 50°C for two minutes. The second step was DNA denaturation and activation of the polymerase at 95°C for ten minutes, followed by 40 cycles of amplification at 95°C for 15 seconds and fluorescence detection at 60°C for 25 seconds. Ramp rate was set to 100% or 1,6 °C/sec.

Table 1. The RT-qPCR thermal cycle program for TREC and KREC quantification.

Step	Time	Temperature	Cycles	Function
1	2 min	50°C	1	UDG
2	10 min	95°C	1	Activation/Denaturation
3	15 sec 25 sec	95°C 60°C	40	Amplification Fluorescence detection

Sensitivity, specificity, positive and negative likelihood ratio and positive and negative predictive values (P/NPV) for both TREC and KREC RT-qPCR method were calculated using the equations 2–5. Inconclusive results (ACTB <1000 copies/µL) and repeated measurements were excluded from the calculations.

Sensitivity: $\frac{true\ positive}{true\ positive + false\ negative}$ (a) Specificity: $\frac{true\ negative}{false\ positive + true\ negative}$ (b)

PPV: $\frac{true\ positive}{true\ positive + false\ positive}$ (c) NPV: $\frac{true\ negative}{false\ negative + true\ negative}$ (d)

Equation 2a-d. Sensitivity, specificity, positive predictive value (PPV) and negative predictive value (NPV) were calculated according to equations 2a-d.

3.6 Peripheral blood mononuclear cells isolation

25 mL of whole blood diluted in PBS was carefully loaded on top of 10 mL Ficoll Histopaque®-1077 (Sigma Aldrich, MO, USA) and centrifuged for 30 minutes at 1600 rpm at RT without brakes. PBMCs were collected from the interphase with a pasteur pipette. PBMCs were washed with 30 mL phosphate buffer saline (PBS) for 10 minutes at 1400 rpm at RT. Supernatant was discarded and cells re-suspended in 30 mL PBS. Cells were counted using trypan blue staining and Countess® automated cell counter (Invitrogen) and calculated with equation 6.

$$live\ cell\ concentration/mL \times sample\ (mL) = total\ number\ of\ cells\ in\ sample$$

Equation 3. Total number of cells in sample was calculated as counted live cell concentration/mL multiplied by the sample volume.

PBMCs were frozen in freezing medium at a concentration of $5 \cdot 10^6$ cells/mL. Samples were frozen using Mr.Frosty (Thermo Fisher Scientific Inc., Waltham, USA) at -80°C and then kept at -197°C in liquid nitrogen until further analysis.

3.7 Flow cytometry analysis

Navios Flow Cytometer (Beckman Coulter Inc., Ireland) was used for flow cytometry analysis using mouse anti-human monoclonal abs (mAb). Staining setup is listed in Table 2. 10^5 events were collected for each sample.

3.7.1 Extracellular staining

50 μL of whole blood or $5x10^5$ of PBMCs were added to each tube. 10 μL of gammagard (0,4 mg/mL) was added to each sample and samples incubated for 10 minutes at RT to prevent unspecific binding of the mAbs. 4 μL of each mAb was added to each tube according to the staining setup. Tubes were incubated at 4°C for 20 minutes in darkness and then lysed with 1 mL of VersaLyse lysing solution (Beckman coulter Inc.) followed by centrifugation at 3500 rpm for five minutes. After removal of the supernatant, samples were washed with 1 mL of PBS with centrifugation at 3500 rpm for five minutes. Supernatant was discarded and 300 μL of FACS staining buffer added to each tube, except for tubes number two. The deposit in tubes two was divided in half, 300 μL of FACS staining buffer added to the other one whereas intracellular staining was performed on the other half. Samples were kept at 4°C in the dark and analysed within four hours of staining.

3.7.2 Intracellular staining

Foxp3/transcription factor staining buffer set (eBioscience, Inc., CA, USA) was used for intracellular staining. Cells were permeabilized with one mL of fixation/permeabilization concentrate and incubated for 40 minutes at 4°C in the dark. Cells were then washed with 2 mL permeabilization buffer and centrifuged at 300 g for 10 minutes. After removal of supernatant, cells were stained with 5 μL of FoxP3 mAb and incubated at 4°C for 30 minutes in the dark. Cells were then washed twice with 2 mL

of permeabilization buffer with centrifugation at 300 g for 10 minutes. 300 μL of FACS staining buffer was finally added to each sample and samples kept at 4°C in the dark and analysed within four hours of staining.

Table 2. Fluorescent-labelled Abs used for cellular staining.

	Flourochrome	Tube 1	Tube 2	Tube 3	Tube 4	Tube 5	Tube 6	Tube 7
FL1	FITC	CD62L	CD127	CD45RA	CD16	α / β	IgD	κ
FL2	PE	CD28	CD25	CD45RO	CD56	γ / δ	IgM	λ
FL3	ECD/ PE-eFluor610	CD45RA		CD38		CD45	CD38	
FL4	PC5/ PerCP-Cy5,5	CCR7			CD203		CD138	
FL5	PC7	CD3	CD3	CD3	CD3	CD3	CD5	
FL6	APC	CD4	FoxP3	CD31	CD4	CD4	CD19	CD19
FL8	AF750 APC-Cy7	CD8	CD8	CD8	CD8	CD8	CD20	
FL9	PB	CD27	CD4	CD4	HLA-DR	CD14	CD27	

3.8 Serum immunoglobulin measurements

Total IgG, IgA and IgM serum Igs were measured in samples from three of the DGS subjects with rate nephelometry on IMMAGE® 800 Immunochemistry System (Beckman Coulter Inc.). Samples were diluted 1:36 for IgA and IgM measurements and 1:216 for IgG measurements. Ig serum levels were calculated according to the dilution factor and reported in g/L values.

3.9 Statistical analysis

Standard curve and TREC, KREC and ACTB quantification were calculated in SDS 2.2, the software for ABI PRISM® 7900HT (Applied Biosystems®). Navios and Kaluza® flow analysis software version 1.2 (Beckman Coulter Inc.) were used for flow cytometry data analysis. Basic calculations were done in Microsoft Excel. All graphs and statistical calculations were made in GraphPad Prism version 5.04 (GraphPad Software, Inc., CA, USA). Mann-Whitney U test was used compare different cell phenotypes between DGS subjects and HC, and p value <0,05 was considered as statistically significant.

4 Results

4.1 DNA elution

DNA concentration in DBS samples from healthy subjects was used to determine the assurance of the DNA elution method. The DNA concentration range was approximately 180–250 ng/µL (one outlier excluded) and the mean DNA concentration was 220 ng/µL (Figure 5).

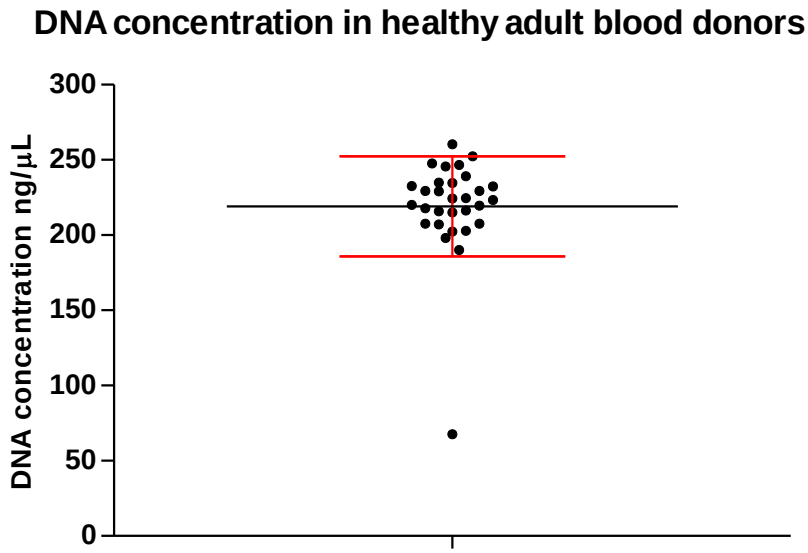

Figure 5. DNA concentration (ng/µL) in samples from healthy adult blood donors. DNA was eluted from neonatal DBS samples and measured with NanoDrop (NanoDrop technologies). Mean value ± SD.

4.2 TREC and KREC RT-qPCR

4.2.1 TREC and KREC RT-qPCR as neonatal screening methodology

The TREC, KREC and ACTB results from the RT-qPCR from all healthy neonatal DBS samples are shown in Figure 6. TREC copies/µL is shown on the x axis, KREC copies/µL on the y axis and the dot sizes are relative to the ACTB concentration (copies/µL). Cut-off values are set as TREC 8 copies/µL and KREC 6 copies/µL and are shown with red lines. Abnormal results are shown as red dots and the axes are logicle scales in order to show the null results. Retested results and results from DGS subjects are excluded from the dataset.

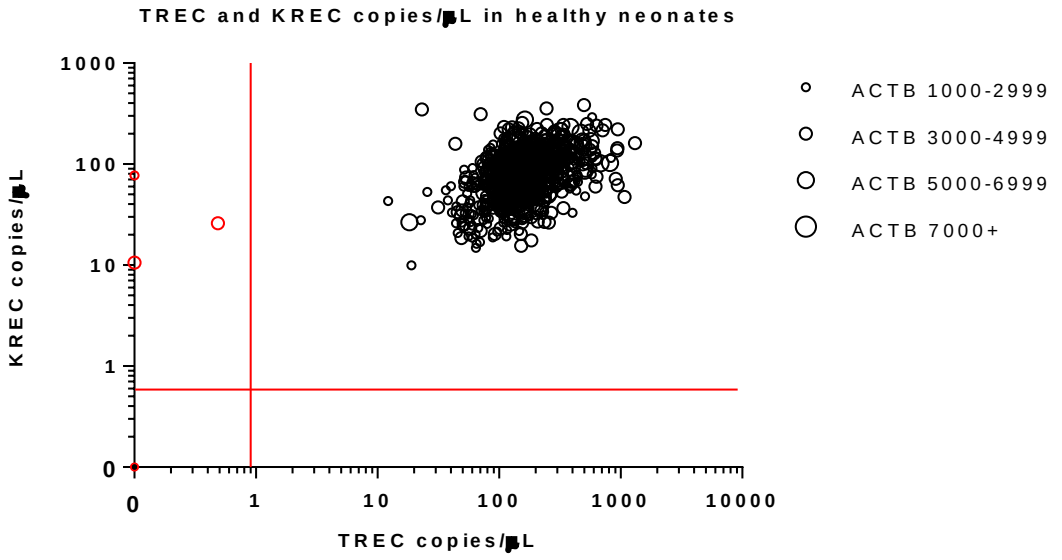

Figure 6. TREC and KREC (copies/µL) in healthy neonates. TREC values are on the x axis, KREC values on the y axis and dot size is relative to the ACTB concentration for each sample. Red lines indicate the cut-off values (TREC 8 copies/µL and KREC 6 copies/µL). n=848.

Results from all healthy neonatal DBS samples were grouped according to normal, abnormal or inconclusive results (Figure 7). 848 neonatal samples were analysed with the RT-qPCR. Three results were abnormal with a TREC value below the cut-off value (8 copies/µL) and ACTB value above the cut-off value (1000 copies/µL), and only four results had inconclusive results with ACTB value below the cut-off value. Only one sample from all the abnormal and inconclusive results remained inconclusive upon retesting. The rate for repeated testing is 0,83%, calculated from these results.

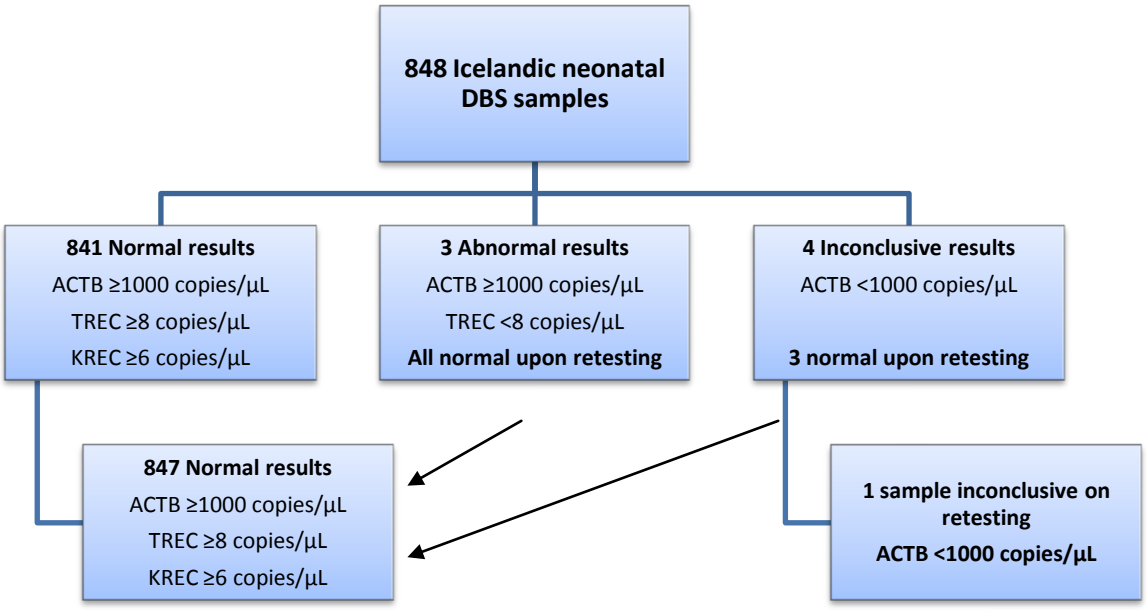

Figure 7. Result summary of neonatal DBS samples. Healthy neonatal DBS samples were grouped into normal, abnormal and inconclusive according to the results. Abnormal and inconclusive results were retested whereas only one appeared to be normal upon retesting.

4.2.2 DGS subjects had low TREC values and normal KREC values

RT-qPCR results for the DGS subjects are seen in Figure 8. The TREC copies/µL is shown on the x axis, KREC copies/µL on the y axis and the dot sizes are relative to the ACTB copies/µL quantity. The axes are logicle scales and the red lines represent the cut-off values for TREC (8 copies/µL) and KREC (6 copies/µL). Results for DGS1, DGS2 and DGS3 were inconclusive with undetectable TREC, KREC and ACTB values. Therefore, the dots for DGS1, DGS2 and DGS3 all emerge at the null point in Figure 7. DGS4, DGS5 and DGS6 results are mean values from a duplicate. These subjects had TREC values below the cut-off value (<8 copies/µL) and normal KREC and ACTB values.

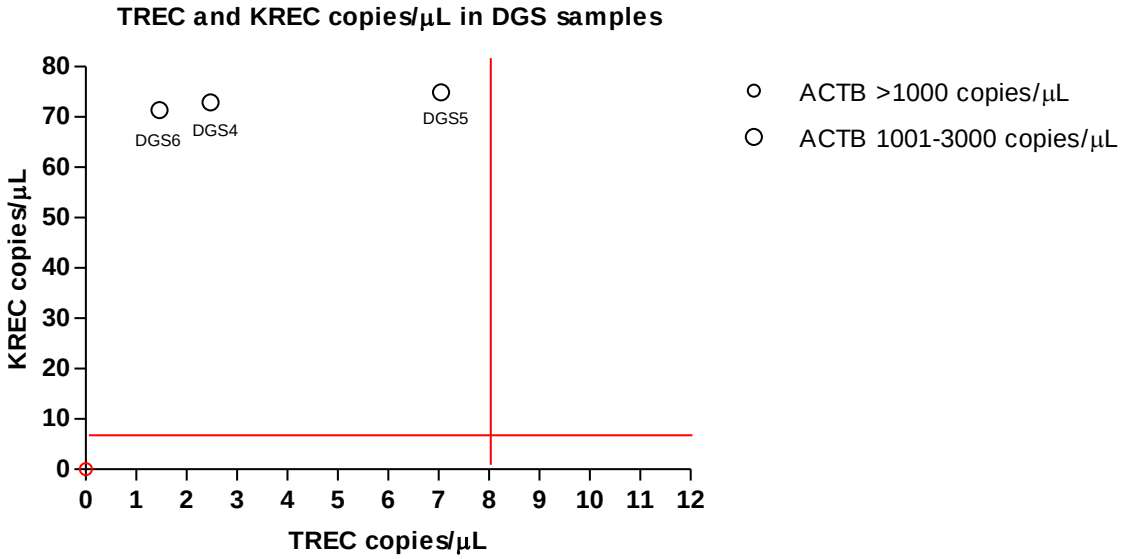

Figure 8. TREC and KREC copies/µL in DGS subjects. TREC values are on the x axis, KREC values on the y axis and dot sizes are relative to the ACTB value per sample. Red lines indicate the cut-off values (TREC 8 copies/µL and KREC 6 copies/µL). n= 6

4.2.3 The quality of the TREC KREC RT-qPCR method

Standard curve was calculated from the five standard samples in each RT-qPCR, and TREC, KREC and ACTB copy numbers evaluated from the standard curve. The range of coefficient of determination (R^2) for the standard curves was 0,9742–0,9993 and the mean was 0,9881 (Figure 9).

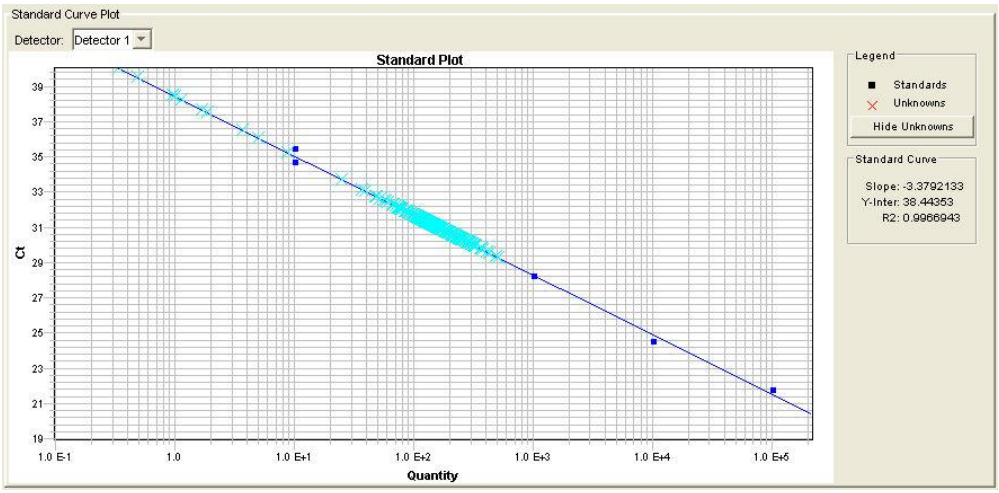

Figure 9. A TREC and KREC RT-qPCR standard curve. Standard curves were calculated from the five standard samples analysed in each RT-qPCR run. R_2 range: 0,9742–0,9993, mean: 0,9881, n=4.

Quality measurements were made for the TREC and KREC RT-qPCR method in order to access the quality and accuracy of the method (Table 3).

Table 3. The quality of the TREC and KREC RT-qPCR method. Sensitivity, specificity, PLR and NLR was calculated in order to access the quality and accuracy of the RT-qPCR method. PLR: positive likelihood ratio, NLR: negative likelihood ratio**.**

	TREC	KREC
Sensitivity	100,00%	100,00%
Specificity	99,65%	100,00%
PLR	285,71	100,00
NLR	0,00	0,00

Control samples were included in every one of the four RT-qPCR run. The mean values for TREC, KREC and ACTB and the expected results are shown in Table 4. Only one out of four BCD results had both sufficient ACTB and TREC values and the one result was inconclusive (<ACTB). Results from the other control samples had expected results.

Table 4. Control measurement results. The control samples results compared to the expected results. TCD: T cell depleted sample, BCD: B cell depleted sample, TBCD: T and B cell depleted sample, NC: Normal control. The sign < indicates results lower than cut-off values and the equal sign (=) indicates results equal or above cut-off values.

	Results (mean, copies/µL)			Expected results		
	TREC	KREC	ACTB	TREC	KREC	ACTB
TCD	0,12 <	189,68 =	1927,05 =	<	=	=
BCD	6,79 <	0,16 <	761,73 <	=	<	=
TBCD	1,28 <	0,37 <	1315,53 =	<	<	=
NC	84,64 =	61,27 =	1786,58 =	=	=	=
Blank	0 <	0 <	0 <	<	<	<

4.3 Leukocyte subpopulations in DGS

4.4 Leukocytes

Lymphocytes were gated using forward scatter (FSC) and side scatter (SSC), monocytes were identified as $CD3^{-}CD4^{+}CD14^{+}$, neutrophils as $CD45^{+}CD14^{lo}$ and eosinophils as $CD45^{+}CD14^{intermediate}$.

As shown in Figure 10 (and Table 9, appendix), no difference was observed in the fraction of the various leukocyte subpopulations when compared to either HC and/or normal reference values. This was also true for total cell numbers (data not shown).

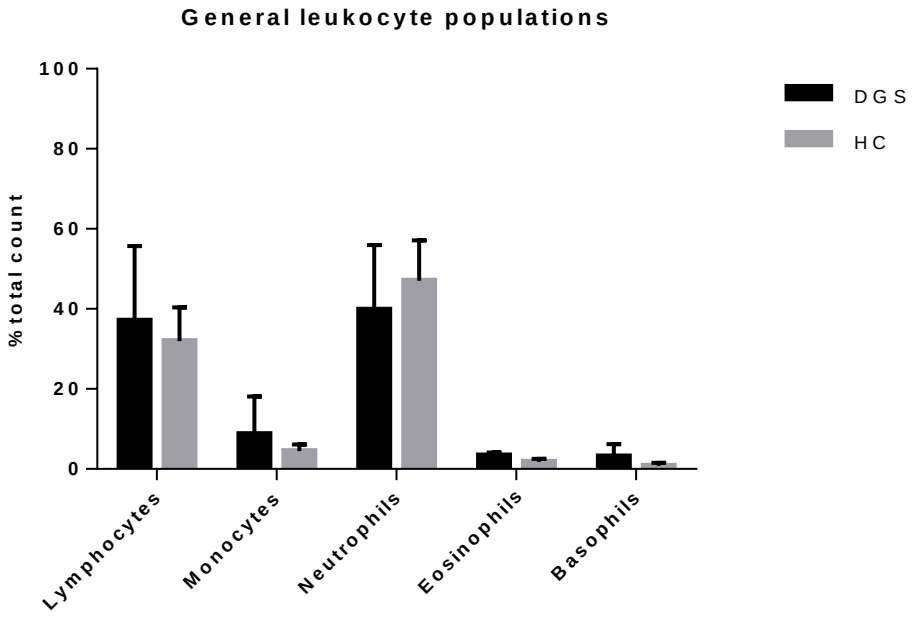

Figure 10. General leukocyte populations in DGS and HC. Lymphocytes were gated on forward scatter (FSC) and side scatter (SSC), monocytes were identified as $CD3^{-}CD4^{+}CD14^{+}$, neutrophils as $CD45^{+}CD14^{lo}$ and eosinophils as $CD45^{+}CD14^{intermediate}$. Mean (%cell count) ±SD, DGS n= 6, HC n=3, Mann-Whitney´s U test.

4.4.1 Lymphocytes

Lymphocytes were gated using FSC and SSC and CD4 T cells identified as CD3+CD4+CD8-, CD8 T cells as CD3+CD4-CD8+ and B cells as CD19+CD20+. No difference was observed in the general lymphocyte populations between DGS and HC (Figure 11 and Table 10, appendix).

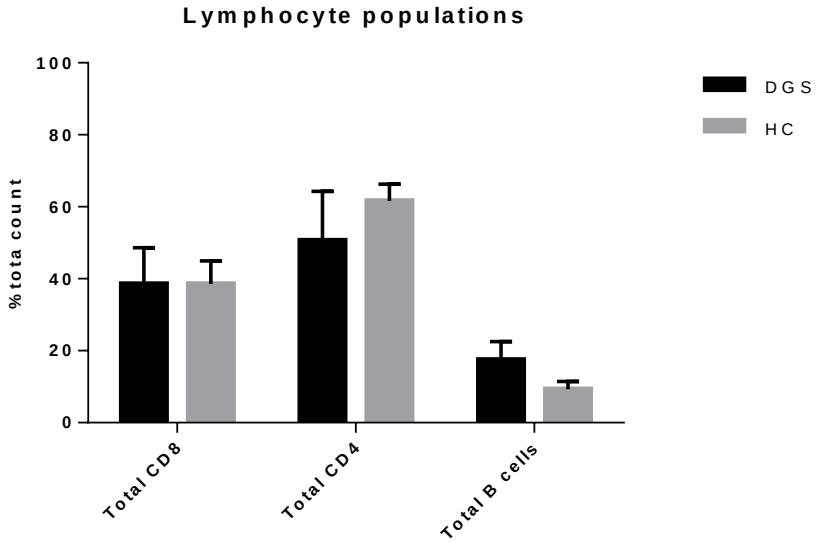

Figure 11. $CD4^+$ T cells, $CD8^+$ T cells and B cells in DGS and HC. CD4+ T cells were identified as CD3C+CD4+CD8-, CD8+ T cells as CD3+CD8+CD4- and B cells as CD19+CD20+. Values are shown as relative size of total cell count. Mean ±SD, DGS n= 6, HC n=3, Mann-Whitney´s U test.

The CD4+ and CD8+ lymphocyte populations were characterized further into subpopulations. Naive T cells were identified as $CD45RA^+CCR7^+$, T_{CM} cells as $CD45RA^-CCD7^+$, T_{EM} cells as $CD45RA^-CCR7^-$ and T_{EMRA} as $CD45RA^+CCR7^+$. T cells were also examined as being early ($CD27^+CD28^+$), intermediate ($CD27^+CD28^-$) or late ($CD27^-CD28^-$) differentiated, regardless of their CD45RA and CCR7 expression. T regulatory cells (T_{regs}) were identified as $CD25^+CD127^-FoxP3^+$. At last, the TCR α/β and γ/δ glycoprotein expression was examined in both $CD4^+$ and $CD8^+$ T cells.

As shown in Table 5 (and Figure 13, appendix), DGS subjects had lower fraction of naive $CD4^+$ T cells and $CD4^+$ T_{EMRA} cells ($p<0,05$). When observing the $CD8^+$ T cell subpopulations, DGS showed lower fractions of $CD8^+$ naive T cells, $CD8^+$ TCM and intermediate differentiated $CD8^+$ T cells. In addition, DGS subjects had higher fractions of CD8+ TEMRA ($p<0,05$, Table 6 and Figure 14, appendix).

Table 5. CD4+ T cell subpopulations in DGS and HC. The mean and range for the relative size of various subpopulations**.** Naive T cells: $CD45RA^{+}CCR7^{+}$, T_{CM}: $CD45RA^{-}CCD7^{+}$, T_{EM}: $CD45RA^{-}CCR7^{-}$, T_{EMRA}: $CD45RA^{+}CCR7$-, early differentiated: $CD27^{+}CD28^{+}$, intermediate differentiated: $CD27^{+}CD28^{-}$, late differentiated: $CD27^{-}CD28^{-}$, T_{regs}: $CD25^{+}CD127^{-}FoxP3^{+}$. DGS n= 6, HC n=3. Mann-Whitney´s U test, p<0,05.

	DGS	HC	P value
$CD4^{+}$ $CD45RA^{+}CCR7^{+}$ naive	13,02	39,03	<0,05
	3,78–26,77	23,33–61,81	
$CD4^{+}$ $CD45RA^{-}CCR7^{+}$ central memory	8,87	16,10	NS
	0,88–18,67	4,71–27,10	
$CD4^{+}$ $CD45RA^{-}CCR7^{-}$ effector memory	11,54	28,66	NS
	5,04–15,91	6,22–41,73	
$CD4^{+}$ $CD45RA^{+}CCR7^{-}$ terminally differentiated effector memory	66,58	16,31	<0,05
	40,83–84,95	7,84–27,62	
$CD4^{+}$ $CD25^{+}CD127^{-}FoxP3^{+}$ T_{regs}	2,8	1,75	NS
	1,46–4,53	0,00–5,24	
$CD4^{+}$ $CD27^{+}CD28^{+}$ Early differentiation	88,35	89,5	NS
	82,84–96,92	86,05–94,09	
$CD4^{+}$ $CD27^{+}CD28^{-}$ Intermediate differentiation	0,07	0,15	NS
	0,01–0,14	0,04–0,30	
$CD4^{+}$ $CD27^{-}CD28^{-}$ Late differentiation	2,81	1,63	NS
	0,02–6,29	0,03–3,98	
$CD4^{+}$ αβ	76,36	39,17	NS
	15,00–97,20	25,22–53,99	
$CD4^{+}$ γδ	0,89	2,91	NS
	0,01–4,13	0,56–7,46	

Table 6. CD8+ T lymphocyte subpopulations. The mean and range for the relative size of various subpopulations. Naive T cells: $CD45RA^{+}CCR7^{+}$, T_{CM}: $CD45RA^{-}CCD7^{+}$, T_{EM}: $CD45RA^{-}CCR7^{-}$, T_{EMRA}: $CD45RA^{+}CCR7$-, early differentiated: $CD27^{+}CD28^{+}$, intermediate differentiated: $CD27^{+}CD28^{-}$, late differentiated: $CD27^{-}CD28^{-}$, T_{regs}: $CD25^{+}CD127^{-}FoxP3^{+}$. DGS n= 6, HC n=3. Mann-Whitney´s U test, p<0,05.

	DGS	HC	P value
$CD8^{+}$ $CD45RA^{+}CCR7^{+}$ naive	1,01	26,44	<0,05
	0,38–1,90	17,26–34,82	
$CD8^{+}$ $CD45RA^{-}CCR7^{+}$ central memory	0,39	1,74	<0,05
	0,10–0,94	0,61–3,43	
$CD8^{+}$ $CD45RA^{-}CCR7^{-}$ effector memory	5,76	17,76	NS
	0,82–17,60	0,71–27,99	
$CD8^{+}$ $CD45RA^{+}CCR7^{-}$ terminally differentiated	92,84	54,07	<0,05
	81,33–98,37	36,02–71,43	
$CD8^{+}$ $CD25^{+}CD127^{-}FoxP3^{+}$ T_{regs}	4,89	N/A	NS
	0,00–18,00	N/A	
$CD8^{+}$ $CD27^{+}CD28^{+}$ Early differentiation	65,32	59,55	NS
	35,99–90,40	44,44–84,21	
$CD8^{+}$ $CD27^{+}CD28^{-}$ Intermediate differentiation	3,99	27,58	<0,05
	0,11–8,12	10,53–47,22	
$CD8^{+}$ $CD27^{-}CD28^{-}$ Late differentiation	13,38	10,09	NS
	2,73–25,68	5,26–16,67	
$CD8^{+}$ αβ	68,02	11,73	NS
	4,43–94,49	5,71–19,63	
$CD8^{+}$ γδ	4,15	6,82	NS
	0,56–12,46	0,65–18,92	

The relative size of RTE ($CD45RA^{+}CD31^{+}$) and TREChi ($CD31^{+}CD38^{+}$) T cell populations was examined in order to correlate the results to the TREC RT-qPCR results. Preliminary data analysis regarding the RTE and $TREC^{hi}$ T cells did not demonstrate any difference in those phenotypes. Naive $CD8^{+}$ T cells ($CD45RA^{+}CD45RO^{-}$) appeared to be lower in DGS subjects compared to the HC (p<0,05, Table 7 and Figure 15, appendix).

Table 7. Naive, recent thymic emigrants and TREC^{hi} T cell populations in DGS and HC. The mean and range relative size of various subpopulations. RTE: recent thymic emigrants, CD45RA^{+}CD31^{+}, TREC^{hi}: CD31^{+}CD38^{+}, naive: CD45RA^{+}CD45RO^{-}. DGS n= 6, HC n=3. Mann-Whitney´s U test, p<0,05.

	DGS	HC	P value
CD4^{+} CD45RA^{+}CD45RO^{-} Naive	34,44	46,71	NS
	24,82–45,68	31,40–59,82	
CD4^{+} CD31^{+}CD45RA^{+} RTE	39,18	34,34	NS
	27,40–55,52	20,72–41,32	
CD4^{+} CD31^{+}CD38^{+} TREC^{hi}	55,24	35,48	NS
	36,98–80,90	23,86–45,65	
CD8^{+} CD45RA^{+}CD45RO^{-} Naive	50,61	68,56	<005
	30,20–65,97	60,96–76,99	
CD8^{+} CD31^{+}CD45RA^{+} RTE	66,88	80,46	NS
	38,49–90,37	67,20–97,90	
CD8^{+} CD31^{+}CD38^{+} TREC^{hi}	56,03	38,07	NS
	33,52–70,52	22,69–58,14	

B lymphocytes were identified as CD19^{+}CD20^{+}. Furthermore, naive B cells were identified as CD27^{-}IgD^{+}, switched memory (SM) B cells were as CD27^{+}IgD^{-} and non-switched memory (NSM) B cells as CD27^{+}IgD^{+}. Plasma cells were identified as CD19^{+}CD20^{-}CD27^{hi}CD38^{hi}CD138^{+}. Both SM and NSM populations were higher in DGS subjects compared to HC (p<0,05, Table 8 and Figure 16, appendix).

Table 8. B cell subpopulations in DGS and HC. The relative size of various subpopulations. Naive: $CD19^{+}CD20^{+}$ $CD27^{-}IgD^{+}$, SM: switched memory $CD19^{+}CD20^{+}$ $CD27^{+}IgD^{-}$, NSM: non-switched memory $CD19^{+}CD20^{+}$ $CD27^{+}IgD^{+}$ and plasma cells $CD19^{+}CD20^{-}CD27^{hi}CD38^{hi}CD138^{+}$. Mean and range, DGS n= 6, HC n=3. Mann-Whitney´s U test.

	DGS	HC	P value
$CD19^{+}CD20^{+}CD27^{-}IgD^{+}$ Naive	78,83	79,52	NS
	71,39–86,39	77,28–82,60	
$CD19^{+}CD20^{+}CD27^{+}IgD^{-}$ SM	5,79	0,56	<0,05
	2,48–9,25	0,32–0,79	
$CD19^{+}CD20^{+}CD27^{+}IgD^{+}$ NSM	11,87	1,69	<0,05
	5,64–17,17	1,48–1,84	
$CD19^{+}CD20^{-}CD27^{hi}CD38^{hi}CD138^{+}$ plasma cells	8,003	2,54	NS
	2,22–14,68	2,12–2,80	
$CD19^{+}CD20^{+}$ kappa†	24,24	11,28	NS
	7,15–33,36	8,28–12,90	
$CD19^{+}CD20^{+}$ lambda†	37,15	30,57	NS
	26,72–45,42	26,47–36,66	

†DGS1, DGS2 and DGS3 excluded from dataset

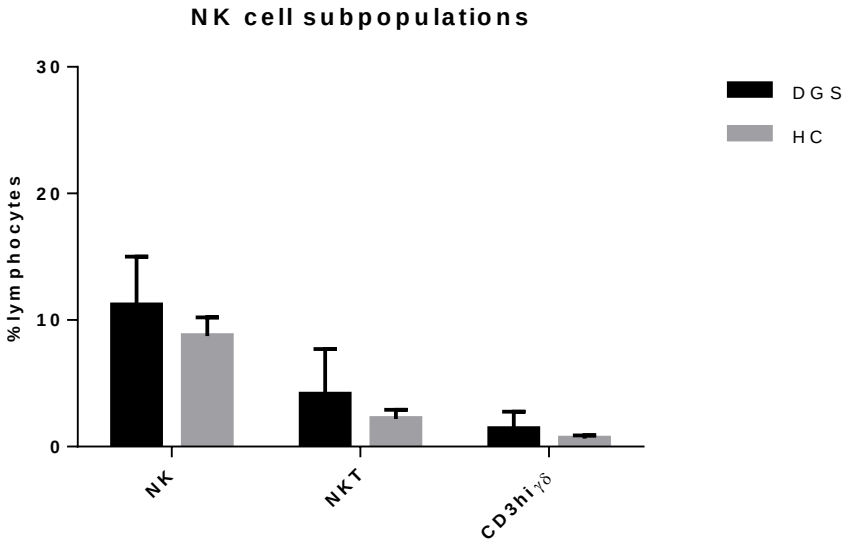

Figure 12. NK cell subpopulations in DGS and HC. NK cells were identified as $CD3^{-}CD56^{+}$, NKT as $CD3^{+}CD56^{+}$ and $CD3^{hi}$γδ as $CD3^{hi}CD56^{+}$.

NK cell subpopulations were examined and NK cells identified as $CD3^{-}CD56^{+}$. NKT subpopulation was determined as $CD3^{+}CD56^{+}$ and $CD3^{hi}$γδ as $CD3^{hi}CD56^{+}$ (Figure 12).

4.5 Serum Ig measurements

Reference interval values for serum IgA, IgG and IgM are age related. Subjects DGS5 and DGS6 had normal serum IgA, IgG and IgM levels. DGS4, however, had slightly reduced serum IgM levels and normal serum IgG and IgA levels (data not shown).

5 Discussion

The aim of this study was to setup a TREC and KREC RT-qPCR method with the possibility to install the method as a neonatal screening program for PID´s. In addition, we wanted to investigate the cellular phenotypes in individuals diagnosed with DGS. The setup of the TREC and KREC RT-qPCR was successful, considering the sensitivity and specificity of the method and various phenotypes were examined in individuals with DGS with a panoramic cellular staining panel for flow cytometry analysis. Thus, the aims of this study are considered to be fulfilled.

5.1 DNA elution

DNA concentration in DBS samples from healthy adult blood donors was high. Purity and quantity measurements with NanoDrop are not the most accurate ones and were only done in order to evaluate if the DNA elution method was sufficient. This DNA elution method is very robust and yields high concentration of DNA which is beneficial for neonatal screening program to minimal the processing time for each sample.

5.2 TREC and KREC RT-qPCR method

The TREC and KREC values in the healthy neonatal subjects in this study seem to be similar to the values the collaborative study has published (Borte et al., 2012). 848 out of 1200 neonatal samples were analysed and the remaining samples will be analysed later this year. Out of these 848 neonatal samples, only three had abnormal results and four samples had inconclusive results. Upon retesting, one sample remained inconclusive and all of the other samples proved to be normal. The reason for the inconclusive results (after retesting) was unsuccessful DNA elution. Therefore, it is necessary to do a DNA elution from a new punch DBS and run the sample again. The three samples that had abnormal results were all normal upon retesting. The reason for abnormal results that appear to be normal upon retesting is not clear. The percentage of neonatal samples that have to be repeated was 0,83%, which is comparable to the previously published studies (Borte et al., 2012), giving rise to the assumption that the RT-qPCR setup was successful.

Three out of the six DGS subjects had inconclusive results where TREC, KREC and ACTB values were all under the cut-off values. The ACTB results indicate unsuccessful DNA elution. These DNA samples were isolated from whole blood collected in vacutainer with heparin anticoagulant and not from a DBS. If DNA is extracted within 6 hours of sample collection, heparin should not inhibit PCR amplification if DNA has been (Lam et al., 2004). Therefore, heparin is not considered as the preventive cause for the RT-qPCR. Unfortunately, retesting these samples was not a possibility. The remaining DGS subjects (DGS4, DGS5 and DGS6) had low TREC values, as expected despite the fact that TREC values decrease with age. Individuals with DGS have been reported to have low TREC and normal KREC values (Borte et al., 2011).

The TREC and KREC RT-qPCR method is very effective as indicated by the quality measurements. These results are comparable to the results from the collaborative parties (Borte et al., 2012). The results from calculated sensitivity, specificity, PPV and NPV were good, indicating the

good accuracy of the method. The sensitivity reveals that all the atypical subjects were determined as abnormal for both the TREC and KREC analysis. The specificity reveals that almost all of the normal subjects were indeed normal for TREC and KREC. The PPV indicates the fraction of all the abnormal results that are indeed abnormal subjects and the NPV reveals the fraction of all the normal results that are indeed normal subjects. Control samples were included in each PCR plate in each RT-qPCR run. In our study, BCD control results were inconclusive in three out of four RT-qPCR experiments. BCD was eluted separately for all of these four experiments. The three inconclusive results are all from the same batch of BCD whereas the one BCD with expected results is from another batch. Our conclusions are that the BCD control sample is defective rather than the DNA elution being unsuccessful in three out of four experiments.

5.3 Flow cytometry analysis

We were able to setup a comprehensive flow cytometry staining panel to examine various cell phenotypes. Such a comprehensive flow cytometry panel with so many different types of fluorescent mAb has a complex compensation and has to be setup correctly.

The cell scattering of the $CD4^+$ and $CD8^+$ T cells, regarding the CD45RA and CCR7 markers, was not similar to cell scatter plots presented in other studies (Koch et al., 2008). Our results showed a large cell population with fluorescence close to zero, thus emerging at the axes on the bivariate plots. The axes were set to logicle scales in order to make these cells more visual. This cell scattering displayed in all DGS results but only in one $CD4^+$ results from HC. This cell scattering might be due to a compensation error, although the compensation was considered successful and should not be the case here.

5.3.1 $CD4^+$ T cell subpopulations

Only two of the $CD4^+$ T cell subpopulations were statistically different between the two groups. The $CD4^+$ naive population was lower in the DGS subjects, as expected where other studies have observed low naive T cells in individuals with DGS (Markert et al., 2004a). The relative size of the CD4+ T_{EMRA} in both DGS and HC is rather unusual and should be maximum 7% of total $CD4^+$ T cells (Schatorje et al., 2011), but was 16% in NC and 67% in DGS. Emphasising our results, the DGS subjects have higher population of $CD4^+$ T_{EMRA} compared to the HC.

5.3.2 $CD8^+$ T cell subpopulations

Difference was observed in the $CD8^+$ Naive, T_{CM}, T_{EMRA} and intermediate differentiated T cell subpopulations. The $CD8^+$ Naive T cell and T_{CM} populations were lower in DGS than in HC, which were within normal range. The T_{EMRA} population in DGS was very high whereas the HC had high but normal population size (Schatorje et al., 2012). The DGS subjects also had lower fraction of the $CD8^+$ intermediate differentiated T cells.

5.3.3 RTE and $TREC^{hi}$ T cell populations

The RTE and $TREC^{hi}$ results from the flow cytometry analysis do not demonstrate any difference between the DGS subjects and the HC. Slightly lower fraction of both RTE and $TREC^{hi}$ T cells in DGS

subjects could have been expected since they all had TREC values below the cut-off values. As said, there was no correlation between the relative size of RTE and $TREC^{hi}$ T cells and the TREC RT-qPCR results.

5.3.4 B cell subpopulations

The SM B cell population has been shown to be lower in individuals with 22q11 deletion syndrome compared to normal controls (Zemble et al., 2010). Considering DGS as 22q11 deletion syndrome, the results from our study are not comparable to the study from Zemble et al. In fact, the comparison of DGS and HC are reversed and the HC seem to have abnormally low relative size of SM B cells. Our results also demonstrate difference in the NSM B cell population which was not observed in this previous study. Although, it should be noted here that the cell count for SM and NSM in the HC were abnormally low.

Even though the kappa and lambda B cell populations in this study do not demonstrate any difference between the DGS and HC, the relative sizes of these populations are rather unusual. Kappa positive B cells should be approximately 60% of total B lymphocytes (Schatorje et al., 2012) but are 24% for DGS subjects and 11% for HC. The results for the relative size of lambda populations are within a normal range. Results from DGS1, DGS2 and DGS3 were excluded from the dataset when lambda and kappa B cells were examined, where no CD19 expression was observed in the results from these subjects and B cell gating strategies impossible.

6 Conclusions

We demonstrated that the TREC and KREC RT-qPCR setup was successful. The method is very robust and effective and thus very convenient as a neonatal screening method. We conclude that the methodology is ready for installation when the time comes for Iceland to join our neighbour countries in PID neonatal screening strategies.

The flow cytometry results demonstrated some differences in T and B cell subpopulations in the DGS subjects compared to the HC. We were not able to correlate the flow cytometry results to the TREC and KREC RT-qPCR results. Our flow cytometry results were more or less comparable to other studies.

References

Agard, E. A., & Lewis, S. M. (2000). Postcleavage sequence specificity in V(D)J recombination. *Mol Cell Biol, 20*(14), 5032-5040.

Almqvist, N., & Martensson, I. L. (2012). The pre-B cell receptor; selecting for or against autoreactivity. *Scand J Immunol, 76*(3), 256-262.

Ameratunga, R., Woon, S. T., Gillis, D., Koopmans, W., & Steele, R. (2013). New diagnostic criteria for common variable immune deficiency (CVID), which may assist with decisions to treat with intravenous or subcutaneous immunoglobulin. *Clin Exp Immunol, 174*(2), 203-211.

Appay, V., van Lier, R. A., Sallusto, F., & Roederer, M. (2008). Phenotype and function of human T lymphocyte subsets: consensus and issues. *Cytometry A, 73*(11), 975-983.

Bains, I., Antia, R., Callard, R., & Yates, A. J. (2009). Quantifying the development of the peripheral naive CD4+ T-cell pool in humans. *Blood, 113*(22), 5480-5487.

Bassing, C. H., Swat, W., & Alt, F. W. (2002). The mechanism and regulation of chromosomal V(D)J recombination. *Cell, 109 Suppl*, S45-55.

Bateman, E. A., Ayers, L., Sadler, R., Lucas, M., Roberts, C., Woods, A., Packwood, K., Burden, J., Harrison, D., Kaenzig, N., Lee, M., Chapel, H. M., & Ferry, B. L. (2012). T cell phenotypes in patients with common variable immunodeficiency disorders: associations with clinical phenotypes in comparison with other groups with recurrent infections. *Clin Exp Immunol, 170*(2), 202-211.

Borte, S., von Dobeln, U., Fasth, A., Wang, N., Janzi, M., Winiarski, J., Sack, U., Pan-Hammarstrom, Q., Borte, M., & Hammarstrom, L. (2012). Neonatal screening for severe primary immunodeficiency diseases using high-throughput triplex real-time PCR. *Blood, 119*(11), 2552-2555.

Borte, S., Wang, N., Oskarsdottir, S., von Dobeln, U., & Hammarstrom, L. (2011). Newborn screening for primary immunodeficiencies: beyond SCID and XLA. *Ann N Y Acad Sci, 1246*, 118-130.

Brandt, V. L., & Roth, D. B. (2004). V(D)J recombination: how to tame a transposase. *Immunol Rev, 200*, 249-260.

Brauninger, A., Goossens, T., Rajewsky, K., & Kuppers, R. (2001). Regulation of immunoglobulin light chain gene rearrangements during early B cell development in the human. *Eur J Immunol, 31*(12), 3631-3637.

Cancrini, C., Romiti, M. L., Finocchi, A., Di Cesare, S., Ciaffi, P., Capponi, C., Pahwa, S., & Rossi, P. (2005). Post-natal ontogenesis of the T-cell receptor CD4 and CD8 Vbeta repertoire and immune function in children with DiGeorge syndrome. *J Clin Immunol, 25*(3), 265-274.

Castiello, M. C., Bosticardo, M., Pala, F., Catucci, M., Chamberlain, N., van Zelm, M. C., Driessen, G. J., Pac, M., Bernatowska, E., Scaramuzza, S., Aiuti, A., Sauer, A. V., Traggiai, E., Meffre, E., Villa, A., & van der Burg, M. (2013). Wiskott-Aldrich Syndrome protein deficiency perturbs the homeostasis of B-cell compartment in humans. *J Autoimmun*.

Chan, A., Scalchunes, C., Boyle, M., & Puck, J. M. (2011). Early vs. delayed diagnosis of severe combined immunodeficiency: a family perspective survey. *Clin Immunol, 138*(1), 3-8.

Chapel, H., Lucas, M., Lee, M., Bjorkander, J., Webster, D., Grimbacher, B., Fieschi, C., Thon, V., Abedi, M. R., & Hammarstrom, L. (2008). Common variable immunodeficiency disorders: division into distinct clinical phenotypes. *Blood, 112*(2), 277-286.

Conley, M. E., Broides, A., Hernandez-Trujillo, V., Howard, V., Kanegane, H., Miyawaki, T., & Shurtleff, S. A. (2005). Genetic analysis of patients with defects in early B-cell development. *Immunol Rev, 203*, 216-234.

Cunningham-Rundles, C. (2012). The many faces of common variable immunodeficiency. *Hematology Am Soc Hematol Educ Program, 2012*, 301-305.

Douek, D. C., McFarland, R. D., Keiser, P. H., Gage, E. A., Massey, J. M., Haynes, B. F., Polis, M. A., Haase, A. T., Feinberg, M. B., Sullivan, J. L., Jamieson, B. D., Zack, J. A., Picker, L. J., & Koup, R. A. (1998). Changes in thymic function with age and during the treatment of HIV infection. *Nature, 396*(6712), 690-695.

Franzson, L., Jónsson, J., Dagbjartsson, A., & Eiríksdóttir, L. Nýburaskimun - upplýsingar til foreldra. from http://www.landspitali.is/klinisk-svid-og-deildir/rannsoknarsvid/erfda--og-sameindalaeknisfraedi/nyburaskimun---upplysingar-til-foreldra/

Hammarstrom, L., Vorechovsky, I., & Webster, D. (2000). Selective IgA deficiency (SIgAD) and common variable immunodeficiency (CVID). *Clin Exp Immunol, 120*(2), 225-231.

Hsieh, M. Y., Hong, W. H., Lin, J. J., Lee, W. I., Lin, K. L., Wang, H. S., Chen, S. H., Yang, C. P., Jaing, T. H., & Huang, J. L. (2012). T-cell receptor excision circles and repertoire diversity in children with profound T-cell immunodeficiency. *J Microbiol Immunol Infect*.

Jacquemin, V., Rieunier, G., Jacob, S., Bellanger, D., d'Enghien, C. D., Lauge, A., Stoppa-Lyonnet, D., & Stern, M. H. (2012). Underexpression and abnormal localization of ATM products in ataxia telangiectasia patients bearing ATM missense mutations. *Eur J Hum Genet, 20*(3), 305-312.

Jawad, A. F., Prak, E. L., Boyer, J., McDonald-McGinn, D. M., Zackai, E., McDonald, K., & Sullivan, K. E. (2011). A prospective study of influenza vaccination and a comparison of immunologic parameters in children and adults with chromosome 22q11.2 deletion syndrome (digeorge syndrome/velocardiofacial syndrome). *J Clin Immunol, 31*(6), 927-935.

Jung, D., & Alt, F. W. (2004). Unraveling V(D)J recombination; insights into gene regulation. *Cell, 116*(2), 299-311.

Kaufmann, S. H. (2007). The contribution of immunology to the rational design of novel antibacterial vaccines. *Nat Rev Microbiol, 5*(7), 491-504.

Kimmig, S., Przybylski, G. K., Schmidt, C. A., Laurisch, K., Mowes, B., Radbruch, A., & Thiel, A. (2002). Two subsets of naive T helper cells with distinct T cell receptor excision circle content in human adult peripheral blood. *J Exp Med, 195*(6), 789-794.

Koch, S., Larbi, A., Derhovanessian, E., Ozcelik, D., Naumova, E., & Pawelec, G. (2008). Multiparameter flow cytometric analysis of CD4 and CD8 T cell subsets in young and old people. *Immun Ageing, 5*, 6.

Kroger, C. J., Flores, R. R., Morillon, M., Wang, B., & Tisch, R. (2010). Dysregulation of thymic clonal deletion and the escape of autoreactive T cells. *Arch Immunol Ther Exp (Warsz), 58*(6), 449-457.

Lam, N. Y., Rainer, T. H., Chiu, R. W., & Lo, Y. M. (2004). EDTA is a better anticoagulant than heparin or citrate for delayed blood processing for plasma DNA analysis. *Clin Chem, 50*(1), 256-257.

Lee, A. I., Fugmann, S. D., Cowell, L. G., Ptaszek, L. M., Kelsoe, G., & Schatz, D. G. (2003). A functional analysis of the spacer of V(D)J recombination signal sequences. *PLoS Biol, 1*(1), E1.

Lee, G. S., Neiditch, M. B., Salus, S. S., & Roth, D. B. (2004). RAG proteins shepherd double-strand breaks to a specific pathway, suppressing error-prone repair, but RAG nicking initiates homologous recombination. *Cell, 117*(2), 171-184.

Lima, K., Abrahamsen, T. G., Foelling, I., Natvig, S., Ryder, L. P., & Olaussen, R. W. (2010). Low thymic output in the 22q11.2 deletion syndrome measured by CCR9+CD45RA+ T cell counts and T cell receptor rearrangement excision circles. *Clin Exp Immunol, 161*(1), 98-107.

Lu, C. P., Posey, J. E., & Roth, D. B. (2008). Understanding how the V(D)J recombinase catalyzes transesterification: distinctions between DNA cleavage and transposition. *Nucleic Acids Res, 36*(9), 2864-2873.

Marie-Cardine, A., Divay, F., Dutot, I., Green, A., Perdrix, A., Boyer, O., Contentin, N., Tilly, H., Tron, F., Vannier, J. P., & Jacquot, S. (2008). Transitional B cells in humans: characterization and insight from B lymphocyte reconstitution after hematopoietic stem cell transplantation. *Clin Immunol, 127*(1), 14-25.

Markert, M. L., Alexieff, M. J., Li, J., Sarzotti, M., Ozaki, D. A., Devlin, B. H., Sedlak, D. A., Sempowski, G. D., Hale, L. P., Rice, H. E., Mahaffey, S. M., & Skinner, M. A. (2004a). Postnatal thymus transplantation with immunosuppression as treatment for DiGeorge syndrome. *Blood, 104*(8), 2574-2581.

Markert, M. L., Alexieff, M. J., Li, J., Sarzotti, M., Ozaki, D. A., Devlin, B. H., Sempowski, G. D., Rhein, M. E., Szabolcs, P., Hale, L. P., Buckley, R. H., Coyne, K. E., Rice, H. E., Mahaffey, S. M., & Skinner, M. A. (2004b). Complete DiGeorge syndrome: development of rash, lymphadenopathy, and oligoclonal T cells in 5 cases. *J Allergy Clin Immunol, 113*(4), 734-741.

Markert, M. L., Hummell, D. S., Rosenblatt, H. M., Schiff, S. E., Harville, T. O., Williams, L. W., Schiff, R. I., & Buckley, R. H. (1998). Complete DiGeorge syndrome: persistence of profound immunodeficiency. *J Pediatr, 132*(1), 15-21.

Markert, M. L., Sarzotti, M., Ozaki, D. A., Sempowski, G. D., Rhein, M. E., Hale, L. P., Le Deist, F., Alexieff, M. J., Li, J., Hauser, E. R., Haynes, B. F., Rice, H. E., Skinner, M. A., Mahaffey, S. M., Jaggers, J., Stein, L. D., & Mill, M. R. (2003). Thymus transplantation in complete DiGeorge syndrome: immunologic and safety evaluations in 12 patients. *Blood, 102*(3), 1121-1130.

Martini, H., Enright, V., Perro, M., Workman, S., Birmelin, J., Giorda, E., Quinti, I., Lougaris, V., Baronio, M., Warnatz, K., & Grimbacher, B. (2011). Importance of B cell co-stimulation in

CD4(+) T cell differentiation: X-linked agammaglobulinaemia, a human model. *Clin Exp Immunol, 164*(3), 381-387.

Massaad, M. J., Ramesh, N., & Geha, R. S. (2013). Wiskott-Aldrich syndrome: a comprehensive review. *Ann N Y Acad Sci, 1285*, 26-43.

Matalon, O., Reicher, B., & Barda-Saad, M. (2013). Wiskott-Aldrich syndrome protein--dynamic regulation of actin homeostasis: from activation through function and signal termination in T lymphocytes. *Immunol Rev, 256*(1), 10-29.

McCusker, C., & Warrington, R. (2011). Primary immunodeficiency. *Allergy Asthma Clin Immunol, 7 Suppl 1*, S11.

McElhaney, J. E., Pinkoski, M. J., & Meneilly, G. S. (1995). Changes in CD45 isoform expression vary according to the duration of T-cell memory after vaccination. *Clin Diagn Lab Immunol, 2*(1), 73-81.

McLean-Tooke, A., Barge, D., Spickett, G. P., & Gennery, A. R. (2011). Flow cytometric analysis of TCR Vbeta repertoire in patients with 22q11.2 deletion syndrome. *Scand J Immunol, 73*(6), 577-585.

Mohamed, A. J., Yu, L., Backesjo, C. M., Vargas, L., Faryal, R., Aints, A., Christensson, B., Berglof, A., Vihinen, M., Nore, B. F., & Smith, C. I. (2009). Bruton's tyrosine kinase (Btk): function, regulation, and transformation with special emphasis on the PH domain. *Immunol Rev, 228*(1), 58-73.

Murphy, K., Travers, P., & Walport, M. (2008). *Janeway´s Immunobiology* (7th ed.). USA: Garland Science, Taylor & Francis Group, LLC.

Nakagawa, N., Imai, K., Kanegane, H., Sato, H., Yamada, M., Kondoh, K., Okada, S., Kobayashi, M., Agematsu, K., Takada, H., Mitsuiki, N., Oshima, K., Ohara, O., Suri, D., Rawat, A., Singh, S., Pan-Hammarstrom, Q., Hammarstrom, L., Reichenbach, J., Seger, R., Ariga, T., Hara, T., Miyawaki, T., & Nonoyama, S. (2011). Quantification of kappa-deleting recombination excision circles in Guthrie cards for the identification of early B-cell maturation defects. *J Allergy Clin Immunol, 128*(1), 223-225 e222.

Neiditch, M. B., Lee, G. S., Huye, L. E., Brandt, V. L., & Roth, D. B. (2002). The V(D)J recombinase efficiently cleaves and transposes signal joints. *Mol Cell, 9*(4), 871-878.

Oskarsdottir, S., Persson, C., Eriksson, B. O., & Fasth, A. (2005). Presenting phenotype in 100 children with the 22q11 deletion syndrome. *Eur J Pediatr, 164*(3), 146-153.

Pandolfi, F., Cianci, R., Cammarota, G., Pagliari, D., Landolfi, R., Conti, P., & Theoharides, T. C. (2010). Recent insights in primary immunodeficiency diseases: the role of T-lymphocytes and innate immunity. *Ann Clin Lab Sci, 40*(1), 3-9.

Pieper, K., Grimbacher, B., & Eibel, H. (2013). B-cell biology and development. *J Allergy Clin Immunol*.

Pierdominici, M., Mazzetta, F., Caprini, E., Marziali, M., Digilio, M. C., Marino, B., Aiuti, A., Amati, F., Russo, G., Novelli, G., Pandolfi, F., Luzi, G., & Giovannetti, A. (2003). Biased T-cell receptor repertoires in patients with chromosome 22q11.2 deletion syndrome (DiGeorge syndrome/velocardiofacial syndrome). *Clin Exp Immunol, 132*(2), 323-331.

Puck, J. M. (2011). The case for newborn screening for severe combined immunodeficiency and related disorders. *Ann N Y Acad Sci, 1246*, 108-117.

Puck, J. M. (2012). Laboratory technology for population-based screening for severe combined immunodeficiency in neonates: the winner is T-cell receptor excision circles. *J Allergy Clin Immunol, 129*(3), 607-616.

Ratts, R. B., & Weng, N. P. (2012). Homeostasis of lymphocytes and monocytes in frequent blood donors. *Front Immunol, 3*, 271.

Routes, J. M., Grossman, W. J., Verbsky, J., Laessig, R. H., Hoffman, G. L., Brokopp, C. D., & Baker, M. W. (2009). Statewide newborn screening for severe T-cell lymphopenia. *JAMA, 302*(22), 2465-2470.

Sallusto, F., Geginat, J., & Lanzavecchia, A. (2004). Central memory and effector memory T cell subsets: function, generation, and maintenance. *Annu Rev Immunol, 22*, 745-763.

Salzer, U., Warnatz, K., & Peter, H. H. (2012). Common variable immunodeficiency - an update. *Arthritis Res Ther, 14*(5), 223.

Schatorje, E. J., Gemen, E. F., Driessen, G. J., Leuvenink, J., van Hout, R. W., & de Vries, E. (2012). Paediatric reference values for the peripheral T cell compartment. *Scand J Immunol, 75*(4), 436-444.

Schatorje, E. J., Gemen, E. F., Driessen, G. J., Leuvenink, J., van Hout, R. W., van der Burg, M., & de Vries, E. (2011). Age-matched reference values for B-lymphocyte subpopulations and CVID classifications in children. *Scand J Immunol, 74*(5), 502-510.

Schatz, D. G., & Swanson, P. C. (2011). V(D)J recombination: mechanisms of initiation. *Annu Rev Genet, 45*, 167-202.

Serana, F., Chiarini, M., Zanotti, C., Sottini, A., Bertoli, D., Bosio, A., Caimi, L., & Imberti, L. (2013). Use of V(D)J recombination excision circles to identify T- and B-cell defects and to monitor the treatment in primary and acquired immunodeficiencies. *J Transl Med, 11*, 119.

Singh, K., Chang, C., & Gershwin, M. E. (2014). IgA deficiency and autoimmunity. *Autoimmun Rev, 13*(2), 163-177.

Staples, E. R., McDermott, E. M., Reiman, A., Byrd, P. J., Ritchie, S., Taylor, A. M., & Davies, E. G. (2008). Immunodeficiency in ataxia telangiectasia is correlated strongly with the presence of two null mutations in the ataxia telangiectasia mutated gene. *Clin Exp Immunol, 153*(2), 214-220.

Starr, T. K., Jameson, S. C., & Hogquist, K. A. (2003). Positive and negative selection of T cells. *Annu Rev Immunol, 21*, 139-176.

Steffens, C. M., Al-Harthi, L., Shott, S., Yogev, R., & Landay, A. (2000). Evaluation of thymopoiesis using T cell receptor excision circles (TRECs): differential correlation between adult and pediatric TRECs and naive phenotypes. *Clin Immunol, 97*(2), 95-101.

Torimoto, Y., Rothstein, D. M., Dang, N. H., Schlossman, S. F., & Morimoto, C. (1992). CD31, a novel cell surface marker for CD4 cells of suppressor lineage, unaltered by state of activation. *J Immunol, 148*(2), 388-396.

Treanor, B. (2012). B-cell receptor: from resting state to activate. *Immunology, 136*(1), 21-27.

van Zelm, M. C., Szczepanski, T., van der Burg, M., & van Dongen, J. J. (2007). Replication history of B lymphocytes reveals homeostatic proliferation and extensive antigen-induced B cell expansion. *J Exp Med, 204*(3), 645-655.

van Zelm, M. C., van der Burg, M., Langerak, A. W., & van Dongen, J. J. (2011). PID comes full circle: applications of V(D)J recombination excision circles in research, diagnostics and newborn screening of primary immunodeficiency disorders. *Front Immunol, 2*, 12.

Verschuren, M. C., Wolvers-Tettero, I. L., Breit, T. M., Noordzij, J., van Wering, E. R., & van Dongen, J. J. (1997). Preferential rearrangements of the T cell receptor-delta-deleting elements in human T cells. *J Immunol, 158*(3), 1208-1216.

Wang, T., Liang, Z. A., Sandford, A. J., Xiong, X. Y., Yang, Y. Y., Ji, Y. L., & He, J. Q. (2012). Selection of suitable housekeeping genes for real-time quantitative PCR in CD4(+) lymphocytes from asthmatics with or without depression. *PLoS One, 7*(10), e48367.

Yel, L. (2010). Selective IgA deficiency. *J Clin Immunol, 30*(1), 10-16.

Yu, S., Graf, W. D., & Shprintzen, R. J. (2012). Genomic disorders on chromosome 22. *Curr Opin Pediatr, 24*(6), 665-671.

Zemble, R., Luning Prak, E., McDonald, K., McDonald-McGinn, D., Zackai, E., & Sullivan, K. (2010). Secondary immunologic consequences in chromosome 22q11.2 deletion syndrome (DiGeorge syndrome/velocardiofacial syndrome). *Clin Immunol, 136*(3), 409-418.

Appendix

Table 9. Leukocyte subpopulations DGS and HC. Lymphocytes were identified with SSC and FSC, monocytes as $CD3^{-}CD4^{+}CD14^{+}$, Neutrophils as $CD45^{+}CD14^{intermediate}$, eosinophils as $CD45^{+}CD14^{+}$ and basophils as $CD14^{-}CD123^{+}$. Values are shown as fraction of the total cell count. DGS n= 3/6, HC n=3. Mann-Whitney´s U test, p<0,05.

	DGS	*HC*	*Ref.values*	*P value*
Lymphocytes	37,06	31,95		NS
	23,08–55,7	21,62–40,39	20–40	
Monocytes	8,67	4,44		NS
	3,46–18,13	3,40–6,10	2–10	
Neutrophils	39,78	47,05		NS
	19,00–55,92	39,03–57,16	40–80	
Eosinophils	3,59	1,78		NS
	2,52–4,11	0,97–2,51	1–6	
Basophils	2,25	1,18		NS
	0,55–7,35	0,21–2,41	<1–2	

Table 10. Lymphocyte subpopulations. Mean values and range for B cells, CD4 and CD8 T cells in DGS and HC. Values are shown as fractions of total cell count. DGS n= 6, HC n=3. Mann-Whitney´s U test, p<0,05.

	DGS	*HC*	*P value*
B cells	17,49	9,25	NS
	8,50–22,51	6,96–11,49	
CD4 T cells	50,64	61,31	NS
	38,69–64,31	54,95–66,27	
CD8 T cells	38,51	38,57	NS
	28,61–48,65	33,55–44,98	

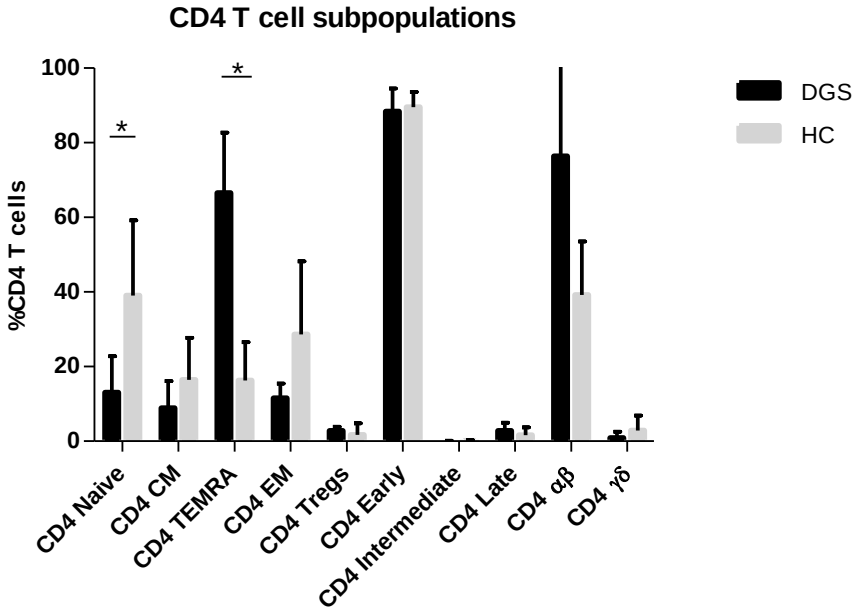

Figure 13. CD4 T cell subpopulations. Naive T cells: $CD45RA^{+}CCR7^{+}$, T_{CM}: $CD45RA^{-}CCD7^{+}$, T_{EM}: $CD45RA^{-}CCR7^{-}$, T_{EMRA}: $CD45RA^{+}CCR7$-, early differentiated: $CD27^{+}CD28^{+}$, intermediate differentiated: $CD27^{+}CD28^{-}$, late differentiated: $CD27^{-}CD28^{-}$, T_{regs}: $CD25^{+}CD127^{-}FoxP3^{+}$. DGS n= 6, HC n=3. Mann-Whitney´s U test, $p<0,05$.

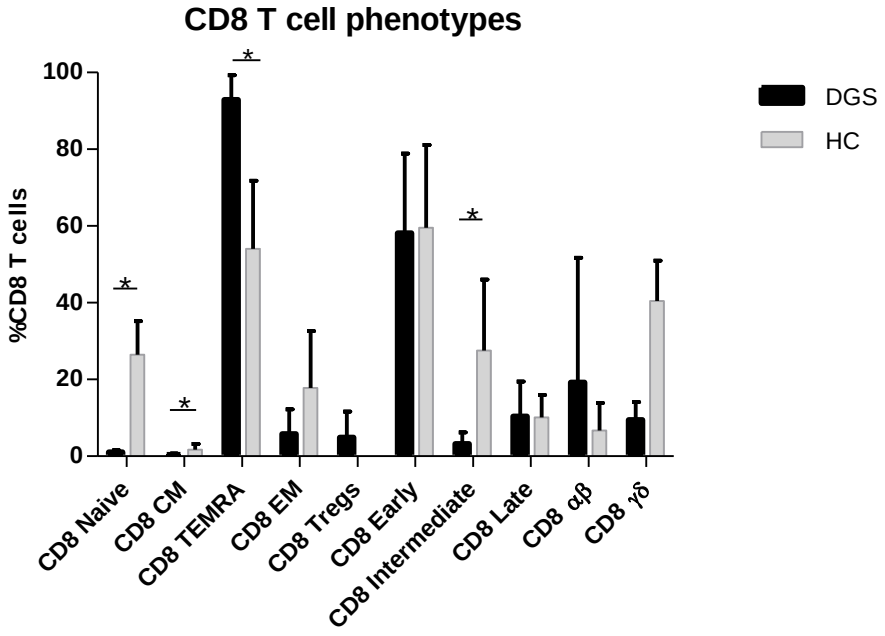

Figure 14. CD8 T cell subpopulations. Naive T cells: $CD45RA^{+}CCR7^{+}$, T_{CM}: $CD45RA^{-}CCD7^{+}$, T_{EM}: $CD45RA^{-}CCR7^{-}$, T_{EMRA}: $CD45RA^{+}CCR7$-, early differentiated: $CD27^{+}CD28^{+}$, intermediate differentiated: $CD27^{+}CD28^{-}$, late differentiated: $CD27^{-}CD28^{-}$, T_{regs}: $CD25^{+}CD127^{-}FoxP3^{+}$. DGS n= 6, HC n=3. Mann-Whitney´s U test, *$p<0,05$.

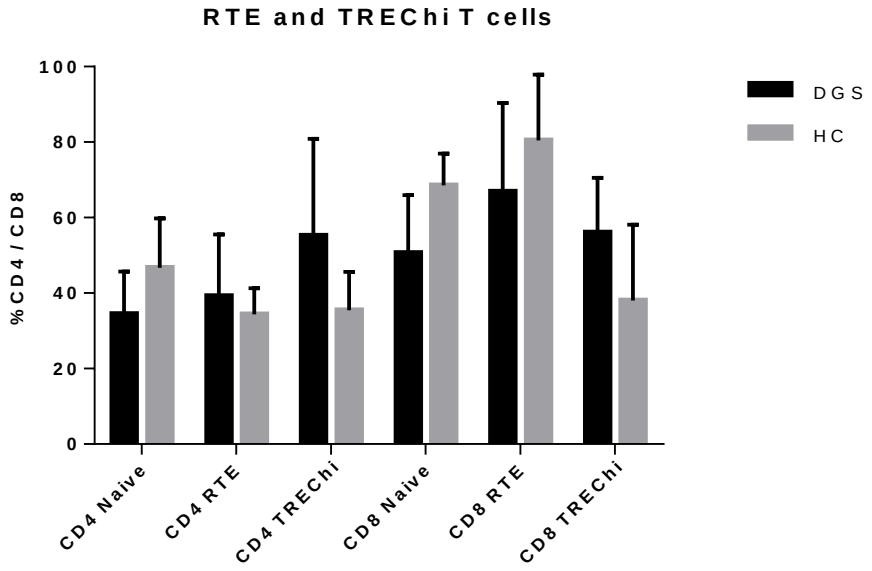

Figure 15. Naive, RTE and TREC^{hi} populations. RTE: recent thymic emigrants, CD45RA^{+}CD31^{+}, TREC^{hi}: CD31^{+}CD38^{+}, naive: CD45RA^{+}CD45RO^{-}. DGS n= 6, HC n=3. Mann-Whitney´s U test, p<0,05.

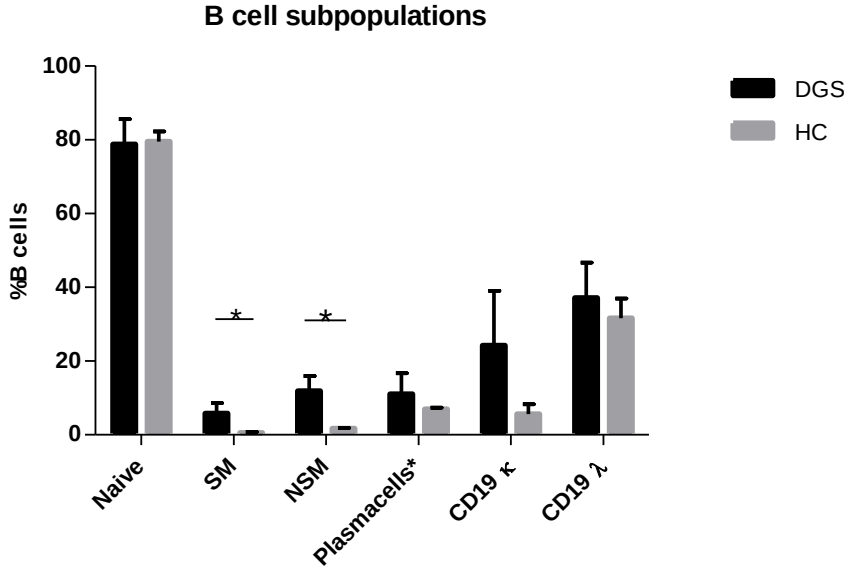

Figure 16. B cell subpopulations in DGS and HC. Naive: CD19^{+}CD20^{+} CD27^{-}IgD^{+}, SM: switched memory CD19^{+}CD20^{+} CD27^{+}IgD^{-}, NSM: non-switched memory CD19^{+}CD20^{+} CD27^{+}IgD^{+} and plasma cells CD19^{+}CD20^{-}CD27^{hi}CD38^{hi}CD138^{+}. Mean and range, DGS n= 6, HC n=3. Mann-Whitney´s U test.